

KERNFORSCHUNGSZENTRUM

KARLSRUHE

Juli 1972

KFK 1658

RCN 172

BLG 471

Institut für Neutronenphysik und Reaktortechnik

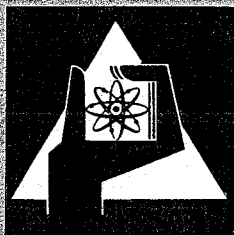
Projekt Schneller Brüter

**Intercomparison of Differential Neutron Spectrometry
Techniques in the MOL- $\Sigma\Sigma$ Fast Assembly**

H. Bluhm, G. Fieg, H. Werle

H. Ames, J.P. Braak, R.J.S. Harry, J. Montizaan

G. De Leeuw-Gierts, S. De Leeuw



**GESELLSCHAFT
FÜR
KERNFORSCHUNG M.B.H.**

KARLSRUHE

THE UNIVERSITY OF CHICAGO
LIBRARY

100 EAST EAST
CHICAGO, ILL.

KERNFORSCHUNGSZENTRUM KARLSRUHE

KFK 1658
RCN 172
BLG 471

Institut für Neutronenphysik und Reaktortechnik
Projekt Schneller Brüter

Intercomparison of Differential Neutron Spectrometry
Techniques in the MOL- $\Sigma\Sigma$ Fast Assembly

H. Bluhm, G. Fieg, H. Werle
H. Ames, J.P. Braak, R.J.S. Harry, J. Montizaan^{*)}
G. De Leeuw-Gierts, S. De Leeuw^{**)}

Gesellschaft für Kernforschung mbH., Karlsruhe
Druck des Inhalts erfolgte durch CEN MOL

^{*)} Stichting Reactor Centrum Nederland

^{**)} Centre d'Etude de l'Energie Nucléaire Mol
Studiecentrum voor Kernenergie Mol

THE UNIVERSITY OF CHICAGO
DIVISION OF THE PHYSICAL SCIENCES
DEPARTMENT OF CHEMISTRY

PH.D. THESIS
SUBMITTED TO THE FACULTY OF THE DIVISION OF THE PHYSICAL SCIENCES
IN CANDIDACY FOR THE DEGREE OF DOCTOR OF PHILOSOPHY
BY
[Name]

DEPARTMENT OF CHEMISTRY
5800 S. UNIVERSITY AVENUE
CHICAGO, ILLINOIS 60637
[Date]

PH.D. THESIS
SUBMITTED TO THE FACULTY OF THE DIVISION OF THE PHYSICAL SCIENCES
IN CANDIDACY FOR THE DEGREE OF DOCTOR OF PHILOSOPHY
BY
[Name]

DEPARTMENT OF CHEMISTRY
5800 S. UNIVERSITY AVENUE
CHICAGO, ILLINOIS 60637
[Date]

PH.D. THESIS
SUBMITTED TO THE FACULTY OF THE DIVISION OF THE PHYSICAL SCIENCES
IN CANDIDACY FOR THE DEGREE OF DOCTOR OF PHILOSOPHY
BY
[Name]

DEPARTMENT OF CHEMISTRY
5800 S. UNIVERSITY AVENUE
CHICAGO, ILLINOIS 60637
[Date]

H. BLUHM, G. FIEG, H. WERLE, H. AMES, J.P. BRAAK, R.J.S. HARRY,
J. MONTIZAN, G. DE LEEUW-GIERTS, S. DE LEEUW
KFK 1658 - RCN 172 - BLG 471 (July 1972)

Abstract The determination of neutron spectra by means of differential spectrometry techniques is a powerful tool to check and evaluate nuclear data. But to reach this objective it is of primary importance to define the confidence that may be attributed to the spectral results wearing errors and uncertainties related to many parameters, such as cross-sections of the reaction used, detection equipment and unfolding codes.

Though only an intercomparison on a large scale can give a valuable estimation of the uncertainties, the differential neutron spectrometry techniques of KFK, RCN and C.E.N./S.C.K., i.e. (n,p) , ${}^3\text{He}(n,p)t$ and ${}^6\text{Li}(n,\alpha)t$ were intercompared in the MOL $\Sigma\Sigma$ fast assembly.

With the care and the precautions taken in the present work and under the experimental conditions described, an agreement of $\pm 5\%$ is generally found between 0,02 and 4 MeV, consequently the same confidence can stand for the neutron spectra measured in similar nuclear and experimental conditions.

H. BLUHM, G. FIEG, H. WERLE, H. AMES, J.P. BRAAK, R.J.S. HARRY,
J. MONTIZAN, G. DE LEEUW-GIERTS, S. DE LEEUW
KFK 1658 - RCN 172 - BLG 471 (juillet 1972)

Résumé La détermination des spectres de neutrons à l'aide de techniques de spectrométrie différentielle permet de vérifier et d'évaluer les données nucléaires. Cette étude ne peut toutefois être entreprise qu'après avoir déterminé la précision sur les résultats expérimentaux, portant des erreurs et des incertitudes liées à un si grand nombre de paramètres (sections efficaces de détection, chaîne électronique d'analyse, codes d'interprétation, etc.) que seule une inter-comparaison à grande échelle permet d'en donner une estimation réelle.

Pour cette raison, une campagne d'inter-comparaison a été effectuée dans l'assemblage MOL $\Sigma\Sigma$, dans lequel furent comparées les techniques de spectrométrie bien établies des centres KFK, RCN et C.E.N./S.C.K. Ces techniques sont basées sur les réactions (n,p) , ${}^3\text{He}(n,p)t$ et ${}^6\text{Li}(n,\alpha)t$.

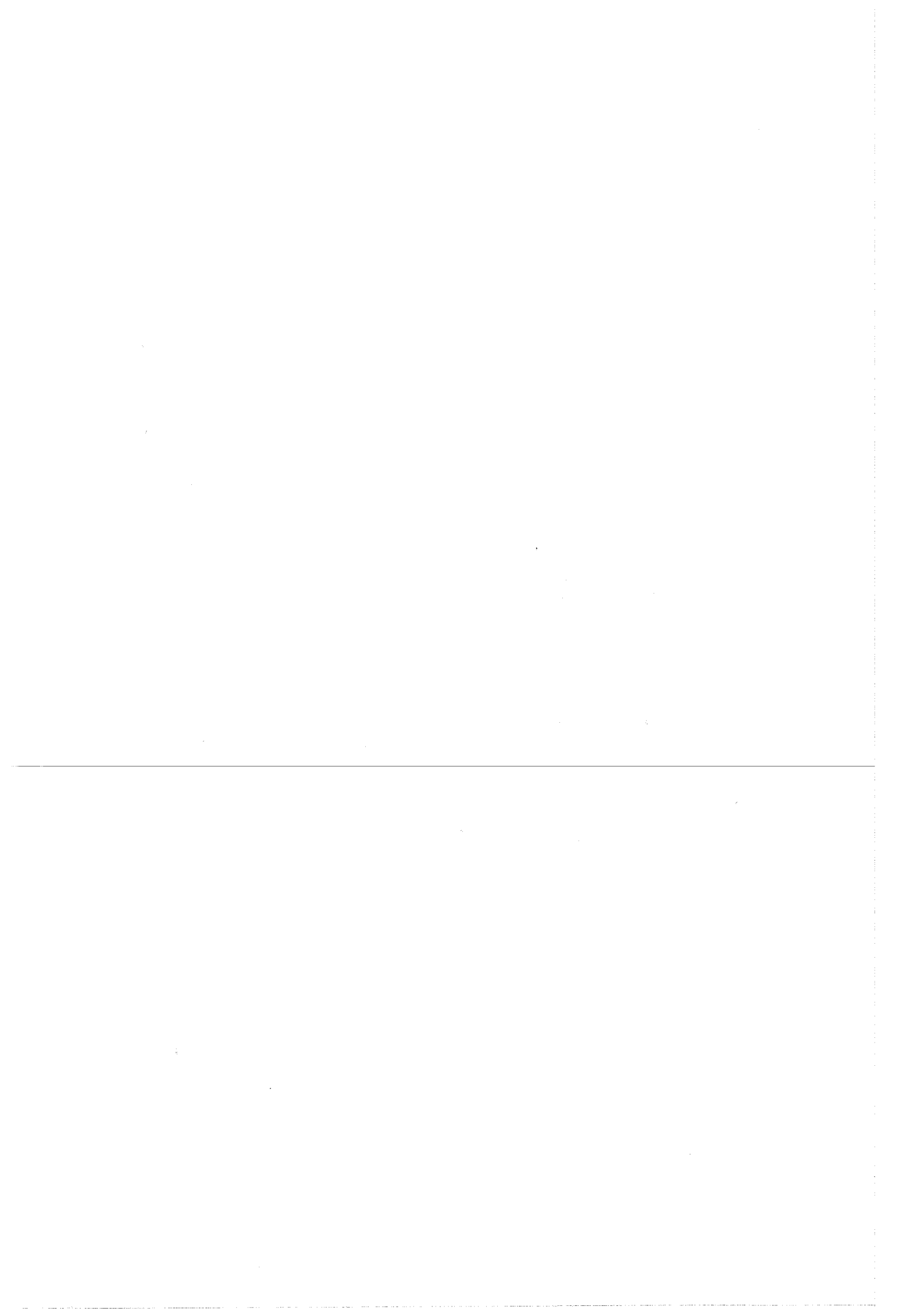
Avec les restrictions et précautions adoptées dans le présent travail et sous les conditions expérimentales décrites, un écart de l'ordre de $\pm 5\%$ entre spectres a été généralement obtenu entre 0,02 et 4 MeV. Cette incertitude peut par conséquent être attendue pour tout spectre de neutrons déterminé dans des conditions nucléaires et expérimentales similaires.

H. BLUHM, G. FIEG, H. WERLE, H. AMES, J.P. BRAAK, R.J.S. HARRY,
J. MONTIZAN, G. DE LEEUW-GIERTS, S. DE LEEUW
KFK 1658 - RCN 172 - BLG 471 (juli 1972)

Samenvatting Het bepalen van neutronenspektra door middel van differentiële spektrometrie-technieken is een belangrijke methode bij het testen en evalueren van nukleaire gegevens. Het is dan ook van primordiaal belang de nauwkeurigheid op deze metingen te kennen. Dit wordt bemoeilijkt door het feit dat de fouten afhangen van vele parameters, zoals werkzame doorsneden van de gebruikte reakties, apparatuur en gebruikte rekenkodes. Enkel een uitgebreide vergelijkende studie laat toe een realistische schatting te bekomen.

Tot dit doel werden de beproefde technieken van respectievelijk KFK, RCN en S.C.K./C.E.N. in de MOL $\Sigma\Sigma$ opstelling toegepast, namelijk : (n,p) , ${}^3\text{He}(n,p)t$ en ${}^6\text{Li}(n,\alpha)t$.

Rekening houdend met de genomen voorzorgen en de beschreven experimentele voorwaarden bedroeg de afwijking in het energiegebied van 0,02 tot 4 MeV, over het algemeen niet meer dan $\pm 5\%$; dit kan dan ook worden aangenomen als onzekerheid op neutronenspektra gemeten onder vergelijkbare nukleaire en experimentele voorwaarden en mits het nemen van dezelfde voorzorgen als in deze studie.



INTERCOMPARISON OF DIFFERENTIAL NEUTRON
SPECTROMETRY TECHNIQUES IN THE MOL- $\Sigma\Sigma$ FAST
ASSEMBLY

H. Bluhm, G. Fieg, H. Werle*
H. Ames, J.P. Braak, R.J.S. Harry, J. Montizaan**
G. De Leeuw-Gierls, S. De Leeuw***

- * Kernforschungszentrum Karlsruhe
- ** Stichting Reactor Centrum Nederland
- *** Centre d'Etude de l'Energie Nucléaire Mol
Studiecentrum voor Kernenergie Mol

Contents

1. Introduction	3
2. Description of the $\Sigma\Sigma$ fast assembly	3
3. Description of the differential neutron spectrometers and associated electronics	4
3.1. KFK spectrometers	4
3.2. RCN spectrometers	6
3.3. C.E.N./S.C.K. spectrometers	8
4. Results	10
4.1. Proton-recoil results	10
4.2. $^3\text{He}(n,p)t$ results	11
4.3. $^6\text{Li}(n,\alpha)t$ results	11
5. Intercomparison of results and techniques	13
5.1. Results	13
5.2. Techniques	13
6. Comparison with theory	15
7. Conclusions	15
References	17
Figure captions	19

1. Introduction

The experimental determination of neutron spectra in fast assemblies is one of the most powerful tools to scan reactor design characteristics. Differences observed between calculated and experimentally deduced neutron spectra may lead to the understanding of the inconsistencies between theoretical and experimental fundamental reactor parameters. Moreover, together with cross-section data consistency tests, the study of the space dependence of the measured spectra and their divergence from the corresponding calculation can improve fundamental cross-sections as well as display the insufficiency of theoretical approximations.

The aim of the present intercomparison work was to define the confidence that might be attributed to the neutron spectrometry techniques. Indeed, the experimental determination of neutron spectra is also subject to uncertainties depending on the nuclear characteristics of the reaction used for the neutron analysis, on the interpretation of the measured spectra involving corrections of several types - nuclear perturbation due to the introduction of the spectrometers-geometry - background - and on unknown systematic errors i.e. related to the electronic equipment, to numerical approximations in the unfolding code, etc.

Although difficult, a systematic study of the parameters influencing a particular spectrometer allows to detect the source and to reduce the errors related to the above-mentioned observations. The deviations resulting from all parameters can be displayed by critically performing the two following steps.

1. The measurement of the same neutron distribution having an isotropic or at least well known angular distribution with several spectrometers, differing either by their type of reaction used for the neutron detection or by the charged particle detector and set-up.

The intercomparison of the results obtained independently with the same or different spectrometers by several specialists in the same nuclear conditions.

2. The study, by a proper choice of the fast assemblies, of the sensitivity of each technique to reactor characteristics such as interfaces, inhomogeneities, angular neutron distributions, nuclear background, γ dose, etc.

The present report deals with the first step, worked out in the spherical natural uranium assembly $\Sigma\Sigma$ driven by the thermal column of the BR1 reactor.

2. Description of the $\Sigma\Sigma$ fast assembly

The $\Sigma\Sigma$ facility is a one-dimensional fast assembly designed to intercompare experimental neutron detection techniques, integral as well as differential ones. Its simple concept makes it easily reproducible in other laboratories and hence permits an intercomparison on international scale.

The secondary standard $\Sigma\Sigma$ is a 5 cm natural uranium shell of 25 cm outer diameter and is located in a spherical cavity of 50 cm diameter hollowed out in the horizontal thermal column of BR1. The thickness of the shell was increased to 5 cm for sufficient degradations of the fission spectrum so as to approach a fast reactor spectrum shape and to shield sufficiently the high γ background of the BR1 reactor. An inner B₄C shell, manufactured by vibrocompaction of boron carbide powder in an aluminium spherical cover, may be introduced in the

uranium shell to cut off the low neutron energy tail of the spectrum. The loading of a spherical proton recoil proportional counter in the complete set-up is shown in Fig. 1.

Physical and nuclear characteristics are extensively described in [1,2]. The fast neutron flux may cover a range of 4 decades i.e. from about $2 \cdot 10^5$ to $2 \cdot 10^9$ n/cm²s, the absolute value of the flux being related to the BR1 reactor power. The neutron spectrum calculated with the DTF IV code, using group cross-sections derived from the Kedak file, is drawn in Fig. 2, together with a KFK 208-groups S8 calculation (cf. §6). The isotropy of the neutron distribution is influenced by the general gradient of the thermal column. The ratio of forward-backward neutron currents deduced from ⁶Li measurements [3] is equal to 1.36, value consistent with other measurements by means of integral techniques. The γ dose in the centre of $\Sigma\Sigma$ corresponding to a fast neutron flux of $6 \cdot 10^8$ n/cm²s obtained at a reactor power of 1 MW was found equal to 350 rad/h.

3. Description of differential neutron spectrometers and associated electronics

3.1. KFK-spectrometers

Proton-recoil proportional counters

Three spherical proportional counters ($\Phi = 3.94$ cm) of the type described by BENJAMIN [4], filled with 2 and 4 atm H₂ and 4 atm CH₄ were used. The reactor power was 70 W for all measurements. The counters were placed in the centre of the $\Sigma\Sigma$ -facility. The reproducibility of the location was within 2 mm. Test measurements were performed with the counters 1 cm outside of the centre. From these measurements, it was concluded that the effect of position reproducibility uncertainty on the measured spectra is below 2 %. The energy calibration was carried out by adding some (0.1 Torr) ³He to the hydrogen filling and 3 % N to the CH₄-filling and observing the corresponding 764 keV or 615 keV peaks respectively. The position of the peaks was checked previously with mono-energetic neutrons from the ⁷Li(p,n)⁷Be-reaction and of a Pb-pile spectrometer [5]. From these it was concluded that the energy E is related to the measured pulse height I by

$$E = \frac{E_c - E_0}{I_c} I + E_0$$

where E_c are the energies of the calibration peaks given above, I_c are the corresponding pulse heights and E_0 equals 0.4 keV for hydrogen and 30 keV for methane.

The spectrum below 100 keV was measured by the 2 atm H₂-counter using the γ -n-discrimination technique [6]. The division of the two pulses is done after digitizing in the ADC's by hardware in the computer. Dead-time losses were about 6 % for the one-dimensional and 15-30 % for the two-dimensional measurements. Details of the electronic system with and without γ -n-discrimination are given in Fig. 3.

The evaluation is done with a code described by BENJAMIN [7], where wall effects are calculated according to the analytical method developed by SNIDOW [8].

Calculated response functions have been compared with measured proton distributions for mono-energetic neutrons. Generally, the measured distributions show larger deformations (from the ideal rectangular shape) than the calculated ones, especially if the wall effects are small [5]. These discrepancies are discussed in 5.2.

³He-semi-conductor-sandwich-spectrometer

Secondly we used a ³He-semi-conductor-sandwich-spectrometer which had recently been developed and tested [9]. This spectrometer differs from the ³He-sandwich-spectrometer used by other authors :

- 1) by a discrimination possibility against γ -background ;
- 2) by the possibility to correct for energy losses of the protons and tritons in the ³He-gas. Therefore, it is possible to extend its useful energy range to 100 keV.

The space between the two circular Si-surface barrier detectors is used as proportional counter. A 40 μ thick counting wire fixed in the midplane between the two semi-conductor diodes forms the anode. The spectrometers have been filled with 2.5 atm ³He and 10 Torr CH₄. The proportional counter is operated at rather low voltages (around 500 volts) leading to moderate gas multiplication factors. The distance between the two Si diodes was 0.6 cm and they had a sensitive area of 200 mm² and a depletion depth of 200 μ .

The spectrometer system only accepts such events which have produced pulses both in the semi-conductor detectors and in the proportional counter, the amplitudes of which exceed certain levels introduced by the electronic system. The possibility of discrimination against γ -background is based on the fact that the specific ionization of Compton electrons (mainly produced in the Si-diodes) is much smaller than that of protons or tritons. Correspondingly, the energy losses of the latter in the ³He gas are considerably larger than that of electrons with the same energy. The electronic system of the spectrometer is shown in Fig. 4. Its fast coincidence unit (resolving time 200 ns) which opens a linear gate considerably reduces the number of summed semi-conductor pulses before adding up the proportional counter pulses. Therefore, pile-up between the broad proportional counter pulses (shaping time 2 μ s) and the summed semi-conductor pulses stretched to 3 μ s is strongly reduced. The threefold sum is multiplied by the proportional counter pulse in a logarithmic computer. The product is generally considerably larger for proton-triton pairs than for electrons. Therefore, proton-triton pulses can be separated from electron pulses by a single-channel analyser.

The energy resolution of the whole system amounted to about 60 keV fwhm. This good resolution is mainly achieved by the addition of the proportional counter pulses, which improves it from about 200 keV to 60 keV. The calibration of the semi-conductor diodes was carried out with a ²³³U- α -source deposited on a thin VYNS foil and placed in an evacuated spectrometer of similar design. By means of this energy calibration, the position (channel number) of the thermal peak of the ³He(n,p)t-reaction was determined and then the amplification of the proportional counter was changed until the experimental position agreed with the calculated one in order to get the right correction for the energy losses in the gas.

From each measured pulse height spectrum such events resulting from (n,p) and (n, α)-reactions in the Si diodes had to be subtracted. This was achieved by another measurement with a similar spectrometer where the ³He-gas had been replaced by ⁴He. Due to the high efficiency, this background was less than 15 % over the whole energy range.

For calculating the neutron spectrum from the measured pulse height distribution it is necessary to know both the $^3\text{He}(n,p)t$ -cross-section and the geometrical efficiency of the spectrometer [9]. The geometrical efficiency has been calculated by a Monte Carlo programme and the results of this programme were checked for different neutron beam entrance directions and different energies between 100 keV and 2 MeV. The agreement between measurement and calculation was satisfactory. Not knowing the exact angular distribution of the fast flux in the $\Sigma\Sigma$ -pile, we used two geometrical efficiencies calculated for different flux distributions. The first efficiency was calculated for an isotropic distribution while in the second case we adopted an anisotropic but energy independent distribution with the following characteristics :

$$\frac{\Phi(0^\circ) + \Phi(180^\circ)}{2\Phi(90^\circ)} = 1.5$$

Comparing spectra evaluated with these efficiencies we find maximum differences of 5 %. The $^3\text{He}(n,p)t$ cross-section used for the evaluation of the spectra is that recommended by Als-Nielsen [10].

3.2. RCN-spectrometers

Proton-recoil spectrometer

The measurements have been done with one spherical counter ($\Phi = 3.94$ cm) of the Benjamin type. The counter was filled with H_2 gas of 4 atmospheres and the energy calibration is obtained from a small plutonium-alpha-source mounted on the anode wire.

A gamma discrimination technique has been used, whereby the difference in slope of the "unshaped" detector pulse, which is about proportional to the specific ionization, is used.

The electronic circuitry (see Fig. 5) consists of a voltage sensitive preamplifier with field effect transistor input to limit the noise level to $25 \mu\text{V}_{\text{eff}}$ at the input. Band width and gain of the preamplifier are 40 MHz and 3 respectively. The signal from the preamplifier is processed in a slow channel yielding the energy information and in a fast channel which yields the specific ionization information. In the fast channel the signal passes a fast amplifier with a gain of 100 and band width of 30 MHz, and is differentiated with $3 \mu\text{s}$ to prevent pile-up without deteriorating the rate of rise of the pulse.

Next the signal passes two D.C. levels of the Pulse Shape Discriminator, which are chosen so as to cover the proportional lower part of the pulse. This passing time is in an exponential way converted into pulse height with the advantage of a better separation between neutrons and gammas [11]. The slow channel consists of an Elscint linear amplifier with $6.4 \mu\text{s}$ pulse shaping.

One Hewlett Packard 1024 channels, 100 MHz ADC digitizes both signals, first the specific ionization signal which is derived at a very early stage of the detector pulse and after that the total energy signal. A switching unit controls the sequence of the signals offered to the ADC. The two digitized signals can be stored in one word, using either 5 and 7, or 5 and 8, or 6 and 6, or 0 and 12 bits for the two signals, respectively. This information is normally stored in an on-line computer (P9202, 16k, 16 bits). For these measurements, however, an interface was made to store the information in the memory of a 4096-channel analyser.

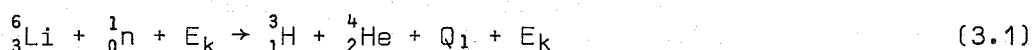
The separately measured gamma spectrum is normalized per energy interval with respect to channel number(s) and contents of the combined (neutron and gamma) measured spectrum and is then subtracted from the combined spectrum.

Next, the remaining contents of the specific ionization channels are added per energy interval, which yields the proton energy spectrum. The neutron spectrum is obtained by unfolding the proton spectrum with a SPEC-4 code.

⁶LiF and ³He semi-conductor sandwich detector

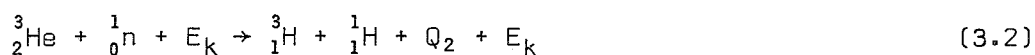
Fig. 6a is a schematic drawing of the Ortec Model 780 ³He fast neutron spectrometer head. For detection of neutrons the spectrometer head is filled with ³He at a pressure of 5 atmospheres. The Ortec model NSB 14 ⁶LiF fast neutron spectrometer head is sketched in Fig. 6b. A further description can be found in reference [12].

Fast neutrons incident on the assembly with a kinetic energy E_k give rise to the reaction :



$$Q_1 = 4.78 \text{ MeV}$$

respectively



$$Q_2 = 0.765 \text{ MeV}$$

The reaction products carry with them the total energy $Q + E_k$ as kinetic energy, because there exists no excited state for the reaction products.

Normally the two silicon surface barrier detectors in the spectrometer head detect both one of the reaction products. The electronic pulses created are equivalent with the kinetic energy of the incident particles. An outline of the electronic amplification chain is given in Fig. 7. The two RCN preamplifiers give their pulses to two Ortec 410 main amplifiers which have a uni-polar and a bi-polar output. The pulses are integrated by a 0.5 μs R.C. integrator and uni-polar respectively bi-polar shaped by one or two delay-lines of 0.8 μs .

The uni-polar pulses are summed, the sum pulses go to the analog to digital converter (ADC) of the multichannel analyser. The bi-polar pulses go to the Ortec model 205 coincidence system. This cross over pick off (COPO) unit gives an output signal if the two input pulses coincide within $\pm 10 \text{ ns}$.

This signal is used to gate the ADC input for the sum pulses. In this way pulses which are not generated at the same moment in both halves of the sandwich are not registered in the multichannel pulse height analyser.

The multichannel pulse height analyser is an Intertechnique and consists of :

- a. CA13 20 MHz ADC for 2048 channels ;
- b. BM96 Memory unit ;
- c. clock unit HC 20 ;

- d. BK21 Driver unit for :
- e. a Tally paper tape puncher.

The neutron spectra are measured with the so-called foreground detector head of the ^6LiF neutron spectrometer in the reactor. The associated electronics are placed in the reactor hall.

After one measurement that can be divided into several periods of some hours, the detector is replaced by the so-called background detector, which has the same initial specifications, but without the evaporated layer of ^6LiF . At equal reactor power and equal time, the background reactions with the silicon of the detectors are measured.

For the ^3He spectrometer head the procedure is the same except that then the same detector head is used for background measurement after evacuation of the ^3He .

The background spectrum is subtracted from the foreground spectrum after a correction for the difference in measurement time (if necessary). The net spectrum is divided by the cross-section for the reaction. For ^3He the cross-section of reference [13] is used, while for ^6Li the cross-section from reference [14] is taken. Besides, due to the fact that not always the two reaction products will be detected in the two halves of the sandwich, the efficiency corrections

$$\epsilon_R = 1 - \frac{7}{12} \sqrt{\frac{E_k}{8 E_k + 44.8}} \quad \text{and} \quad \epsilon_R = 1 - \sqrt{\frac{E_k}{9 E_k + 9.24}}$$

are applied respectively to the ^6Li and ^3He spectra.

3.3. C.E.N./S.C.K. spectrometers

Proton-recoil proportional counters

A spherical proportional counter of the Benjamin Type [4] filled, either with 1 and 2 atmospheres H_2 , or 2 or 4 atmospheres CH_4 , was used to determine the neutron spectrum ; 3 % N_2 was added to both filling types.

A mean energy of 580 keV for the distributions of protons emitted by the thermal $^{14}\text{N}(n,p)^{14}\text{C}$ reaction was considered for energy calibration together with a pulse generator calibration.

The partial neutron spectra obtained with the different gas fillings were partly normalized by the overlapping method ; some measurements being performed in steps over a large period of time, the precision in gas pressure and/or reactor power was insufficient for normalization based on count rates.

Spectra recorded at reactor powers of successively 30, 50 and 70 Watts were compared. No difference within the statistically allowed deviations were observed. The same conclusion could be drawn from the measurements done with CH_4 filling and using B_4C shells with different entrance hole diameters, i.e. 27 mm used for the proton recoil and ^3He measurements and 14 mm used for the ^6Li measurements.

The electronic set-up is reported in Fig. 8.

For the 1 and 2 atmospheres H_2 fillings the γ -n discrimination technique was used to determine the spectrum below 100 keV. The pulse shape discrimination method applied consists in the two-parameter analysis of the energy signal in conjunction with its time derivative. The latter is obtained as the stretched

output of a fast differentiating amplifier, following the preamplifier. The proton recoil spectra were also interpreted by means of the code described by Benjamin [7] and the Snidow [8] subroutine.

⁶Li spectrometry

The ⁶Li spectrometer was manufactured at C.E.N./S.C.K. using either Ortec or home-made detectors. The ⁶LiF is evaporated on one of the detectors, and the distance between both detectors is taken sufficiently large (≥ 7 mm) as to avoid energy dependent loss corrections, due to the angle between the emitted α and triton pair [15], in the analysed energy interval. The detection surfaces were positioned parallel to the general gradient of the thermal column. The neutron spectrum is deduced from the simultaneous analysis of the E_t and $E_\alpha + E_t$ parameter [3]. The background, being rather high in the recording of the $E_\alpha + E_t$ spectrum, must be measured. As observed in earlier measurements, when measuring the background by replacing the ⁶Li sandwich by a new solid state sandwich without Li deposit, one can not be sure of the exact importance and shape of the background to be subtracted.

Wrong background estimation may lead to a too hard spectrum as in [16] or more seldom to a softer one. Indeed, the variations in the detector responses, such as calibration - resolution - depletion depth, due to crystal damages incurred during irradiation, can not all be monitored. Therefore, in the present measurements, a new method was used by which, indirectly through the inverse current and spectrum analysis, an adequate background correction could be assured.

A deposit of 0.1 μm LiF is evaporated on one of the high resolution detectors ; the E_t and $E_\alpha + E_t$ spectra are measured. Only the E_t spectrum is used to determine the neutron spectrum in the very low energy range, from about 3 keV up to 200 keV. A second deposit of 0.6 μm LiF is then evaporated on the same detector and the same measurements are repeated. The second E_t spectrum, with much higher statistics, allows to determine the spectrum up to 700 keV. From 400 keV up to the highest energy limit, the neutron spectrum is deduced from the $E_\alpha + E_t$ spectrum obtained by subtracting the measurements performed with both deposit thicknesses.

The electronics are scheduled in Fig. 9.

The energy resolution of the $E_\alpha + E_t$ spectrum was equal to 240 keV FWHM, it was equal to 33 keV for the E_t spectrum measured with the 0.1 μm deposit, and to 60 keV with the 0.7 μm deposit. Due to the particular $E_t(E_n, \theta = 0^\circ)$ function, where θ is the triton emission angle with regard to the neutron direction [17], lower neutron energy validity limits of 3 and 8 keV might be expected.

Two unfolding codes were successively used for the interpretation of the E_t spectra ; one written by H. Deckers [18] is a general least square unfolding code, the second (UCLIS), written by S. De Leeuw [19] is a specialized code (using implicitly reaction characteristics and a priori information) and interpreting simultaneously the $E_\alpha + E_t$ and E_t spectra. Results of the UCLIS code are reported in 4.3, no discrepancies being observed within the error margin with the results of the least square unfolding code. Due to the poor statistics in the present E_t measurement performed with a 0.1 μm deposit, technique intercomparison conclusions rely on the 0.7 μm deposit results.

The first code is based on a semitheoretical description of the differential angular cross-sections $\frac{d\sigma}{d\Omega}(n,\alpha)$, using parameters calculated by J.C. Bleuet et al. [20] normalized to the Schwarz, Strömberg and Bergström [21] $\sigma(n,\alpha)$ cross-sections, the second one uses a semitheoretical description of the shape of the response functions only. The ENDF/B I file [22] was used to interpret the $E_\alpha + E_t$ spectrum and was taken as reference for the normalization of the neutron spectra deduced from the E_t spectra. In a second step the ENDF/B III set and a re-evaluated cross-section, compared in Fig. 10 to both ENDF/B sets were used.

4. Results

4.1. Proton recoil results

- All GfK measurements were done at 70 W reactor power. Therefore, the runs with the different counters could be normalized over the number of hydrogen atoms in the counter without any arbitrary constants. Below 400 keV the data are from the 2 atm H₂ counter, between 400 and 700 keV from the 4 atm H₂ counter and above 700 keV from the 4 atm CH₄ counter. In the overlapping energy regions the results of the different counters agree generally within the statistical uncertainties.

- In Fig. 11 the RCN results are given of three measurements, carried out at 2900 V.

The first measurement has been done at 70 Watt reactor power and the second measurement, carried out immediately after the first one, at a power of 30 Watt. The results agree within the error margin.

All other measurements have been done at 30 Watt, due to a low count rate. The third measurement, at the end of the measuring period, gives again the same values, except in the last two energy intervals.

The fourth measurement was at 3300 V and was normalized to the theoretical spectrum from 100 to 400 keV. This gives the same results as a normalization in this energy region between this and the mean value of the three preceding measurements. The agreement between the three preceding measurements with each other is better than with this one, especially at the beginning and at the end of the overlapping energy region. However, the greatest difference in this region is still within 2 or 3 standard deviations.

At the lower part, there is an overlap with the fifth measurement at 3500 Volt. A normalization between these two measurements in the energy range from 53 - 68 keV gives the same results as a normalization of the fifth measurement to the theoretical spectrum in the range from 21.5 - 46.5 keV.

- The C.E.N./S.C.K. neutron spectrum below 25 keV is deduced from the 1 atmosphere H₂ measurements. Discrepancies reaching $\pm 15\%$ were observed in the 2 atmosphere H₂ results between 10 and 30 keV, the mean flux in this region being about 20% lower than the one deduced from the 1 atmosphere measurements. In a first step to build up the neutron spectrum above 30 keV the 2 atmosphere H₂ results were used up to 579 keV and normalized between 450 and 600 keV to the 4 atmosphere CH₄ results.

New H₂ measurements showed rather large discrepancies with the older one above about 300 keV. Therefore the neutron spectrum reported here consists of the 2 atmosphere H₂ results up to 320 keV, and the 4 atmosphere CH₄ above this limit. Both spectra were normalized by means of the 2 atmosphere CH₄ measurement,

the region of overlap considered with the H₂ results ranging from 250 up to 400 keV. Normalization between the 4 and 2 atmosphere CH₄ results is based on the hydrogen content of the counter.

Fig. 12 reports the GfK, RCN and C.E.N./S.C.K. proton recoil results, normalized between 25 keV and 1.2 MeV (GfK - C.E.N./S.C.K.) and between 25 keV and 800 keV (RCN - C.E.N./S.C.K.).

4.2. ³He-results

The spectra deduced with the KfK and RCN ³He spectrometers as described in 3.1 and 3.2 are drawn in Fig. 13. The spectra were normalized between 1.26 and 5.01 MeV. Beside the resolution, both ³He techniques differ largely in the relative importance of the background spectrum; consequently lower level energy limit and discrepancies between both spectra are most likely related to the background correction. The large discrepancies between the RCN and KfK results cannot be explained by the different cross-sections used for the evaluation, this accounts for only a plus-minus 8 % error in the 1 to 5 MeV region.

4.3. ⁶Li-results

Fig. 14 compares the spectra deduced from the E_α + E_t RCN by means of the BNL 325 cross-section set and C.E.N./S.C.K. measurements deduced by means of the ENDF/B I cross-sections. Normalization was performed between 0.64 and 3.9 MeV. The systematic discrepancies observed cannot find an explanation in the differences between both cross-section sets; above 2.5 MeV differences even do not exceed a few per cent.

Because of the dispersion of the measured ⁶Li(n,α)t cross-section, resulting most from the presence of the ~ 250 keV resonance (5/2-), the C.E.N./S.C.K. E_t and E_α + E_t spectra were also interpreted with two other cross-section data sets as explained in 3.3. Large discrepancies are observed in Fig. 15 between the derived spectra [23]:

The choice of the detection geometry eliminating energy dependent loss corrections, the ratio of the fast neutron flux, between 10 keV and 4 MeV, to the thermal neutron flux measured with the same spectrometer centered on a plexiglass support in the cavity without ΣΣ could also be deduced using the three cross-section sets. Results are reported in Table I.

Table I

	Exp.			Calc.
	ENDF/B I	Preferred cross-section	ENDF/B III	
$k_1 = \frac{\int_{8.1\text{keV}}^{4\text{MeV}} \Phi(E_n) dE_n}{\Phi_{\text{th}}}$	0.754	0.859	0.908	0.680
$\frac{k_1 \text{ exp.}}{k_1 \text{ theor.}}$	1.11	1.26	1.34	1
$k_2 = \frac{\int_{0.4\text{MeV}}^{4\text{MeV}} \Phi(E_n) dE_n}{\Phi_{\text{th}}}$	0.349	0.394	0.409	0.338
$\frac{k_2 \text{ exp.}}{k_2 \text{ theor.}}$	1.03	1.17	1.21	1

5. Intercomparison of results and techniques

5.1. Results

Having in mind and relying on the remarks of § 4, Fig. 16 compares for clarity purposes three spectra respectively deduced from the RCN and KfK(n,p), the KfK ^3He and the C.E.N./S.C.K. ^6Li measurements.

Good agreement is observed between the proton recoil and the KfK ^3He results. The differences observed between the ^3He spectra of Fig. 13 are consequently to be attributed to insufficient performances, in the present nuclear conditions, of the classical solid state ^3He counter at least below ~ 4 MeV.

The importance of discrepancies observed between the ^6Li measurements below ~ 500 keV depends of course largely on the cross-section used. The good agreement between the proton recoil results and their agreement with ^3He up to 1 MeV supports the shape of the presently adopted cross-section leading to better consistency with $\frac{d\sigma}{d\Omega}$ experimental data.

Due to the fact that the C.E.N./S.C.K. ^6Li spectrum results from one experiment and that, as a consequence, no parameters are injected because of normalization and/or electronics, one may rely on the results obtained below 30 keV; response functions uncertainties can not explain the trend of the discrepancies observed with the other experimental and theoretical data of Fig. 2. This trend is even more pronounced in the high E_t resolution measurement but, as earlier mentioned, with lower statistical accuracy. Between 0.500 MeV and 3 MeV, the agreement between the ^6Li C.E.N./S.C.K. and ^3He KfK results lies within the cross-section error margin. This might indicate, if the real ^6Li and ^3He cross-sections lie effectively within the above-mentioned error margin, that the differences observed between the two ^6Li spectra may result from a different behaviour of the RCN solid state sandwiches consequently to irradiation damage occurred during earlier Stek experiments [26].

Between 3 and 4 MeV the ^6Li results are systematically lower than the ^3He . Several reasons may be put forward, but due to the ^6Li cut off and the ^3He spectral shape above 4 MeV, it is impossible to determine with certainty the origin of the discrepancy.

A systematic difference is observed between the ^3He and ^6Li results at about 1.8 MeV, energy at which corresponds a hump in the cross-section data of the ^6Li as well as the ^3He reaction. Though cross-section precision for the two reactions is estimated to be 10 %, discrepancies may not be attributed to technical parameters.

To remove the doubt in the neutron spectrum in the 2 MeV region, either more precise cross-sections or measurements with an other detection method are needed. A variant of the De Leeuw proton recoil counter [24], that allows to approach a 4π proton detection [25] was constructed to determine the spectrum between 0.5 and 5 MeV. Interpretation of the measurements are under way.

5.2. Techniques

The most important and evident drawbacks are enumerated for each technique hereafter.

a) Proton recoil proportional counter

- Low upper energy limit.

- A set of different counters has to be used to cover a large energy range.

Area normalization of the spectra from different counters (as is used on some cases here) is not an adequate procedure. Normalization should be done over the number of hydrogen atoms in the counter with the help of an independent reactor power monitor. Precise dead-time knowledge over the entire detection system is then absolutely needed.

- Possible errors in the low energy region where pulse shape discrimination is necessary. The reasons for noticed discrepancies are not yet clear. Possible explanations are : insufficient performance of the electronic equipment, inadequate p-correction and finally (below 10 keV for H₂) insufficient knowledge of the behaviour of W (energy loss per ion pair).
- Discrepancies between measured and calculated mono-energetic responses. Generally, measured responses show larger distortions from the ideal rectangular shape. Normally it is assumed that the discrepancies are due to a low energy neutron background in the measurements (scattering in the target and surrounding materials). But the other possibility, that some assumptions made in the calculations (for example, no dead volume in spherical counters) are not adequate, should be kept in mind.

b) ³He spectrometer

- To obtain trustable measurements, necessity to introduce a third counter leading to higher electronic complexity.
- Efficiency calculations depending on neutron distribution parameters because of the unfavourable reaction characteristics

$$E_t \rightarrow 0 \quad \text{if} \quad E_n \rightarrow \infty$$

$$\text{and } \theta + \phi \rightarrow 90^\circ \quad \text{if} \quad E_n \rightarrow \infty \quad \text{with} \quad \theta + \phi = f(\theta)$$

c) ⁶Li spectrometer

- Insufficient cross-section knowledge.
- Low efficiency, leading to a need of a continuous survey of the measurement because of the fast neutron irradiation damage induced in the solid state detectors.
- Rather high background corrections to be performed with a solid state sandwich spectrometer of identical characteristics of the one used for the spectrum measurement.

d) Remarks valid for all techniques

- Complexity.
- Accelerator calibrations are not necessarily an absolute tool to assure correct reactor measurement interpretation. Mono-energetic responses must be considered with much care before applying them to unfold reactor spectra.

The presently most relevant advantages of the three techniques are :

- for the (n,p) spectrometry : cross-section knowledge, counter stability and possible attainable lower validity energy limit ;
- for the ³He technique : cross-section knowledge, efficiency and possible absolute flux determination if the angular neutron distribution is known ;
- for the ⁶Li technique : energy range covered and possible absolute flux determination in any neutron distribution and angular flux measurements.

6. Comparison with theory

The spectrum calculated by means of the DTF IV code is compared to the experimental spectra in Fig. 17. From 0.02 up to 6 MeV experiment and theory agree within $\pm 15\%$. The systematic deviations observed in group 4 may be related to the inelastic cross-section shape [Kedak version 1968]. This has been confirmed by a 208 group calculation (Fig. 19) using an inelastic scattering cross-section, which has been derived from a depleted uranium metal exponential experiment [27] and which is about 30% lower than the Kedak cross-section [1970] around 1.6 MeV.

Between 46.5 keV and 0.800 MeV the mean energy of the experimental spectrum is higher than the theoretical DTF IV one.

It is hard to explain the discrepancies between theory and experiment in the low energy region only by uncertainties of the ^{238}U capture cross-sections. The sensitivity to changes of this cross-section are displayed in Fig. 19; the relative changes of the capture cross-section between both 208 group calculated spectra rise up to 30% below 30 keV.

Next to the ^{238}U neutron cross-section data, too many other parameters are involved, e.g. cross-sections of other elements, wall return calculations, hypothesis on the driver, theoretical approximations, etc., to be able to draw definitive conclusions on the origin of the observed discrepancies. The KfK 208 group calculations have also been performed to make sure that the 35 keV and 90 keV structures observed in all measured E_t spectra and drawn in Fig. 18 could effectively be attributed to neutron interactions with the aluminium cladding of B₄C. The other structures observed in the high resolution E_t spectrum are probably due to interactions with the spectrometer materials.

7. Conclusions

~~The results of the extensive comparison measurements made with different techniques in the $\Sigma\Sigma$ -facility are summarized as follows.~~

- The ratio of the normalized fluxes (integrated over broader energy intervals, Fig. 17) of the following techniques: (n,p), $^3\text{He}(n,p)t$ with γ ,n-discrimination and $^6\text{Li}(n,\alpha)t$ measuring the E_t and $E_\alpha + E_t$ distribution in a single run (Table II) is generally within $\pm 5\%$ equal to one over the whole energy range.

From a consideration of the main contributions to the experimental uncertainties we conclude that this figure holds generally for similar systems, i.e. for systems

- with comparable n, γ -ratio and angular dependence of the neutron field;
- with a neutron spectrum which decreases steadily above about 1.5 MeV to zero at about 10 MeV;
- where the detector counting rates can be kept below adequate levels.

Furthermore, because the $\pm 5\%$ refers to three independent techniques, we conclude that this figure is also a measure for the discrepancies to be expected between the true spectrum and the experimental results received with the well-established techniques.

Table II Energy ranges and accuracies of (broad group fluxes) for the well-established techniques

Techniques	Energy range (MeV)	Accuracy % (Broad group fluxes)
Proton recoil proportional counter	0.02 - 1.5	
⁶ Li-spectrometer (E _α + E _t and E _t distribution)	0.02 - 4	± 5 % (except for group 0.046 to 0.1 MeV)
³ He-spectrometer with γ,n-discrimination	0.1 - 6	

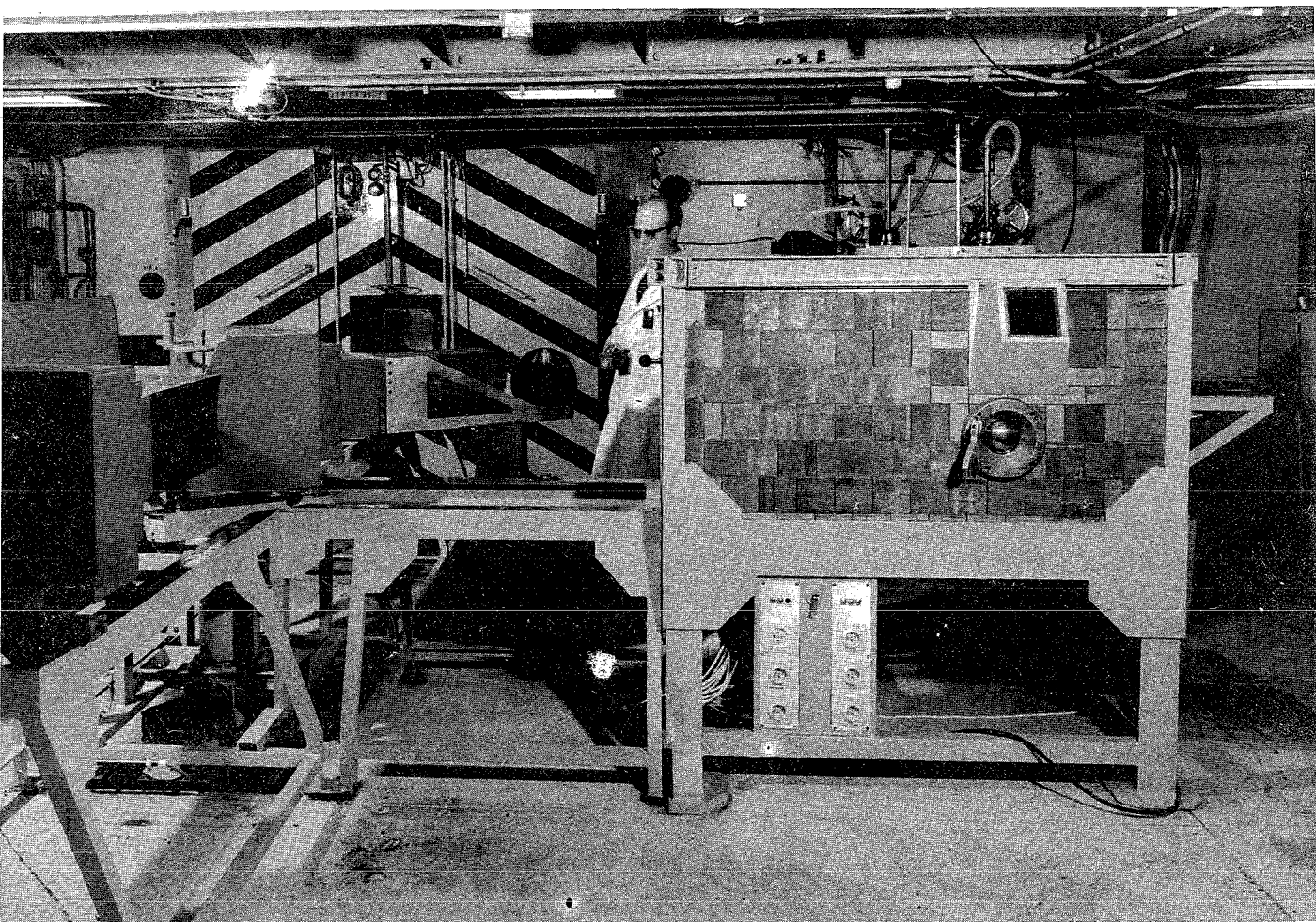
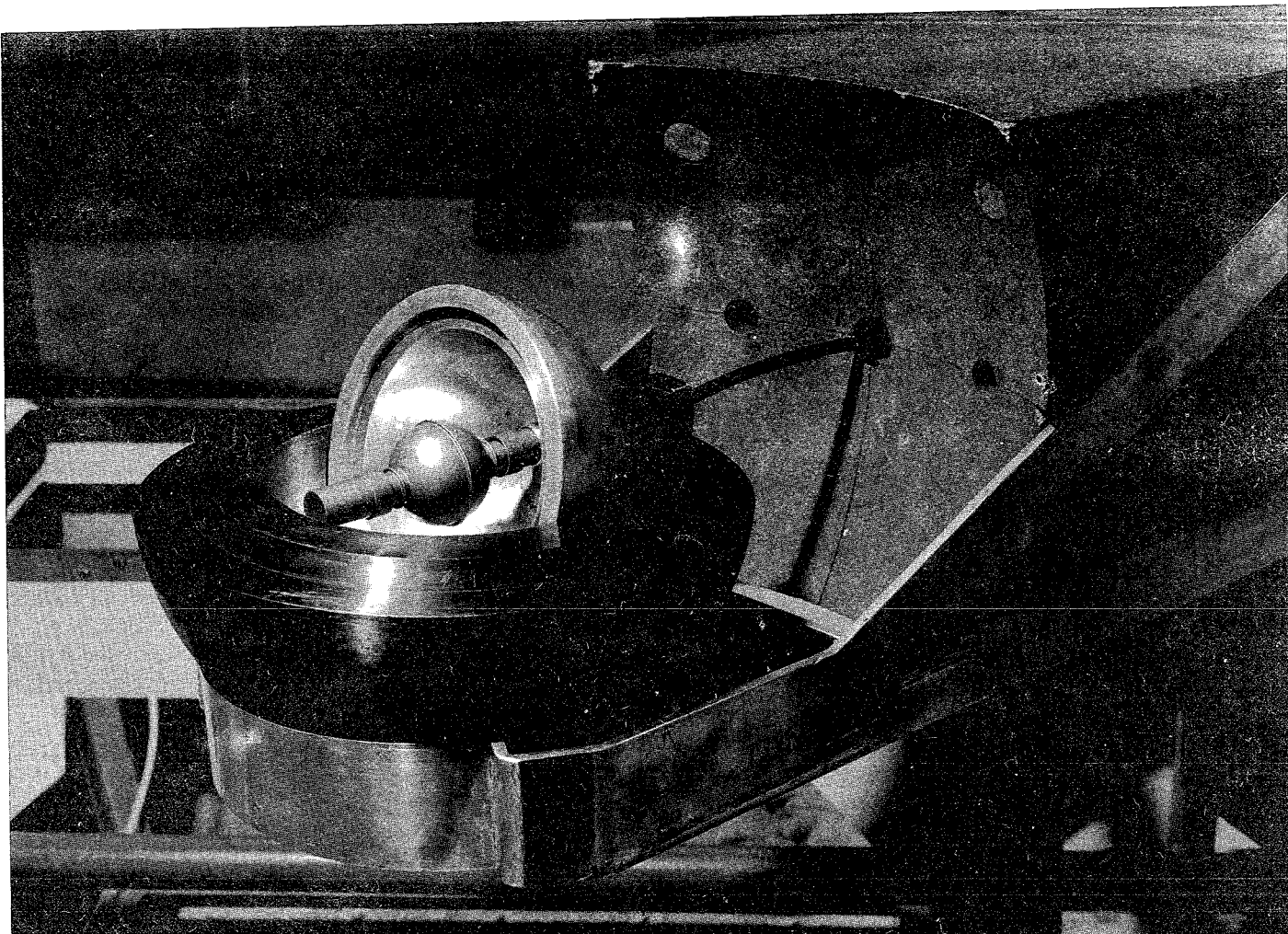
References

- [1] Fabry, A., De Leeuw, G., De Leeuw, S., De Coster, M.
EACRP Meeting (1971)
- [2] De Leeuw-Gierts, G., De Leeuw, S.
Internal Report (1970)
- [3] De Leeuw-Gierts, G., De Leeuw, S.
BLG 450 (1970)
- [4] Benjamin, P.W. et al.
AWRE NR2/64 (1964)
- [5] Werle, H.
KfK-External Report INR-4/70-25, ORNL-tr-2415 (1970)
- [6] Bennett, E.F.
Nucl. Sci. Eng. 27 (1967) 16
- [7] Benjamin, P.W. et al.
AWRE N° 09/68 (1968)
- [8] Snidow, N.L.
BAW-TM-442 (1965)
- [9] Bluhm, H.
KfK 1270/2, p. 121-2 (1970)
- [10] Als-Nielsen, J.
CCDN-NW/6 (1967)
-
- [11] Frumau, C.F.A. and Lautenbag, C.
Nuclear Electronics, Int. Symp. Versailles (1968) Paris 68, p. 101
- [12] Ortec Instruction manual silicon surface barrier detector
Oak Ridge Technical Enterprises Corporation (1964)
- [13] Langner, I., Schmidt, J.J., Woll, D.
Eur 3715 e , EANDC(E)-88U, KfK 750
- [14] BNL 325 Second Edition, supplement N° 2
- [15] De Leeuw-Gierts, G., De Leeuw, S.
BLG 428 (1968)
- [16] De Leeuw-Gierts, G., De Leeuw, S.
Annual Scientific Report, 1970 BLG 460 p. 1-6
- [17] Gierts, G.
Reactor Sci. Tech. 17 (1963) 121
- [18] Deckers, H.
Radn Meas. in Nucl. Power 1966, p. 259-269

- [19] De Leeuw, S.
BLG to be published
- [20] Bluet, J.C., Fort, E., Leroy, J.L.
1964, Internal Rep. Centre d'Etudes Nucléaire de Cadarache, SMNF 64/04
1965, Proc. Int. Conf. on the study of Nuclear Structure with Neutrons,
Antwerp (Amsterdam : North-Holland)
- [21] Schwarz, S., Strömberg, L.G., Bergström, A.
FOA4 Rap A 4393, 411 Stockholm (1964)
- [22] Battat, M.E., Dudziak, D.S., La Bauve, R.J.
LA-3695-MS (1967)
- [23] De Leeuw-Gierts, G., De Leeuw, S.
To be published
- [24] De Leeuw-Gierts, G., De Leeuw, S.
BLG 454 (1971)
- [25] De Leeuw-Gierts, G., De Leeuw, S.
Annual Scientific Report 1971
- [26] Braak, J.P., Harry, R.J.S.
RCN report, to be published
- [27] Bluhm, H.
Spectrum measurements in a depleted uranium metal block for investigation
of discrepant ^{238}U cross-sections
To be published
-

Figure captions

- Fig. 1 Out-of-pile view of the $\Sigma\Sigma$ facility
- Fig. 2 Computed neutron spectra in the centre of the $\Sigma\Sigma$ facility
- Fig. 3 KfK proton-recoil proportional counter electronics
- Fig. 4 KfK ^3He -semi-conductor electronics
- Fig. 5 RCN proton-recoil spectrometer two parameter set-up with BM96 memory block
- Fig. 6 Schematic drawing of model NSB 14 ^6LiF and model 780 ^3He fast neutron sandwich spectrometer head
- Fig. 7 RCN electronic system used with semi-conductor sandwich detectors
- Fig. 8 C.E.N./S.C.K. proton-recoil proportional counter electronics
- Fig. 9 C.E.N./S.C.K. ^6Li semi-conductor electronics
- Fig. 10 $^6\text{Li}(n,\alpha)t$ cross-sections
- Fig. 11 RCN neutron spectrum measurement with a proton-recoil spectrometer
- Fig. 12 (n,p) spectrometry results
- Fig. 13 $^3\text{He}(n,p)t$ spectrometry results
- Fig. 14 $^6\text{Li}(n,\alpha)t$ spectrometry results
-
- Fig. 15 C.E.N./S.C.K. $^6\text{Li}(n,\alpha)t$ results
Comparison of the neutron spectra deduced by means of three different cross-section sets
- Fig. 16 Comparison of the RCN and KfK (n,p) KfK $^3\text{He}(n,p)t$ and C.E.N./S.C.K. $^6\text{Li}(n,\alpha)t$ results
- Fig. 17 Comparison of the computed neutron spectrum with the experimental spectra grouped in the theoretical energy intervals
- Fig. 18 E_t distribution in the centre of $\Sigma\Sigma$
- Fig. 19 Comparison of experimental and 208-group calculated spectra



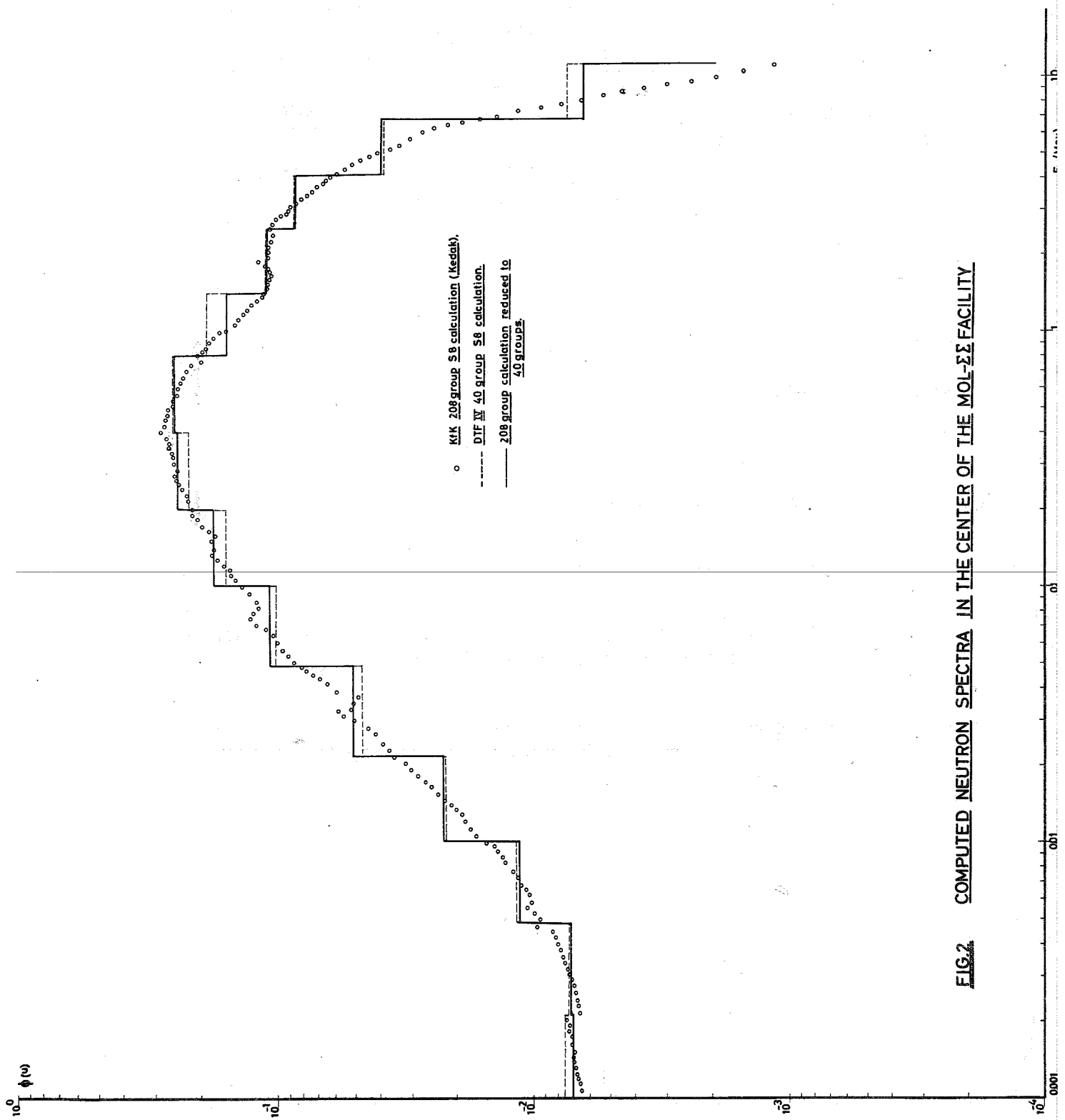
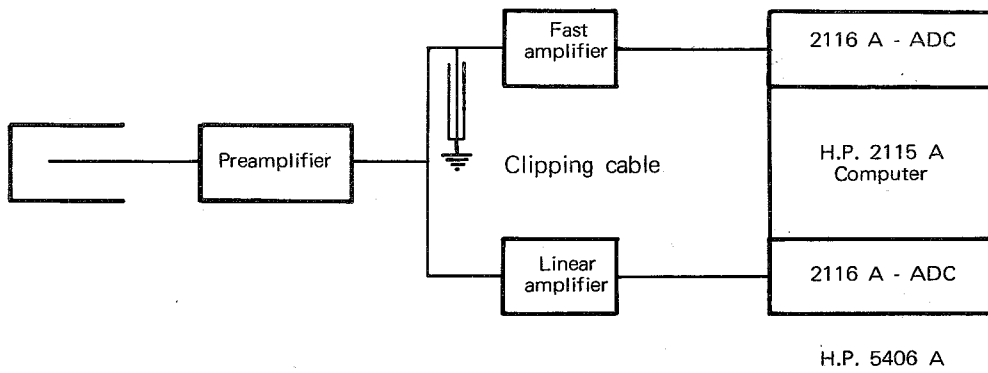


FIG. 2. COMPUTED NEUTRON SPECTRA IN THE CENTER OF THE MOL-ΣΣ FACILITY

Fig. 3. KFK proton-recoil proportional counter electronics



Preamplifier : Two-stage, voltage sensitive FET (gain 50, rise time 30 ns)

Clipping cable : RG58/U-200 ns

Fast amplifier : HEWLETT-PACKARD 5582 A (Integration time 200 ns) +
CANBERRA Pulse Stretcher Model 1463

Linear amplifier : 1-dim. : HVL Model L-120

Counter	Int.	Diff.
2H ₂ , 4H ₂	4 μs	5 μs
4CH ₄	2 μs	2 μs

2-dim. : ORTEC Select. Active Filter Amplifier Model 440 A, Shaping Time 4 μs +
ORTEC Baseline Restorer Model 438, active mode

Nuclear Data Acquisition System : HEWLETT-PACKARD 5406 A consisting of two 2116 A - ADC's
(time-to-peak 5 μs) and a 2115 A (8k, 16 bits) - Computer.

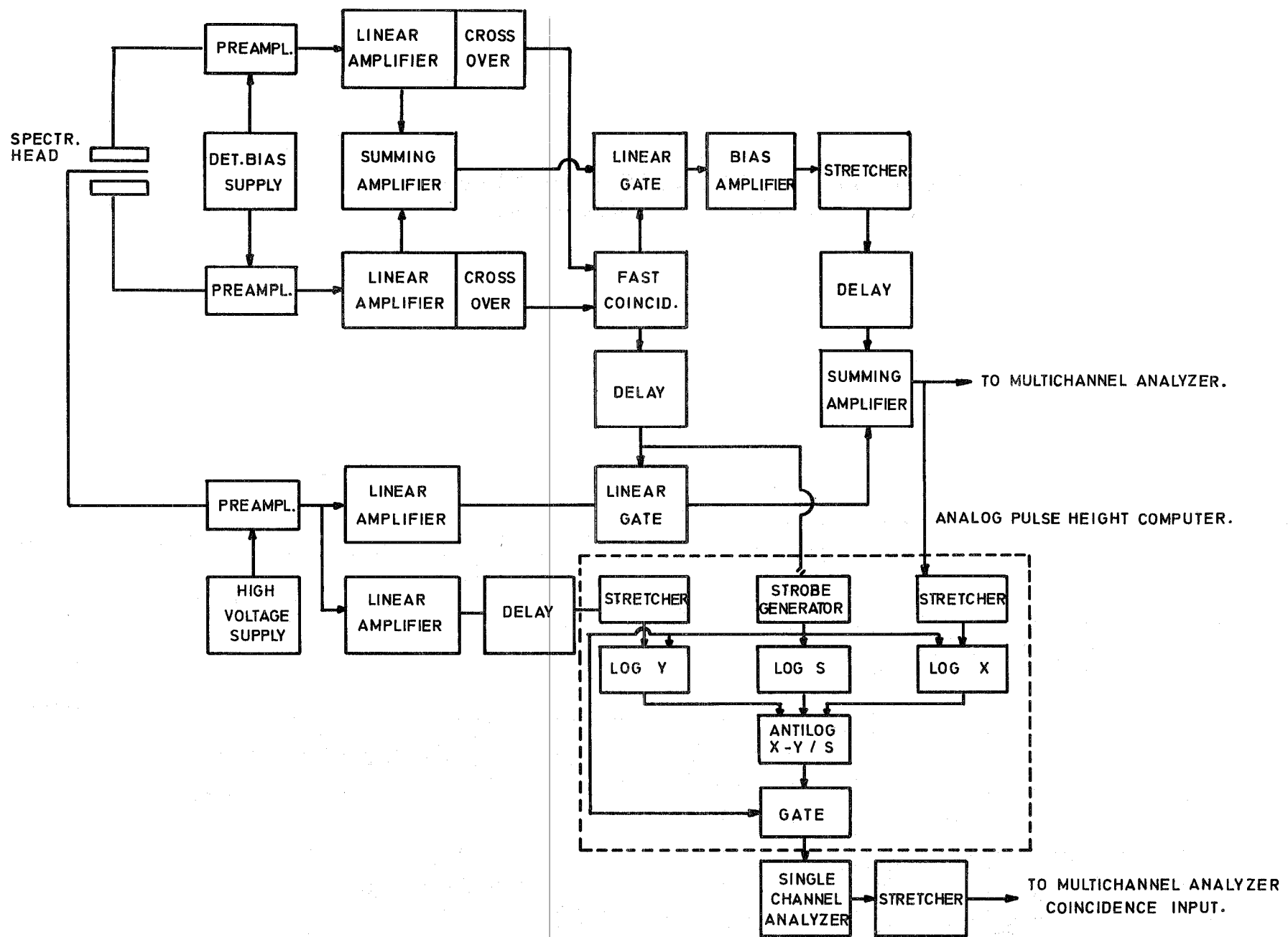
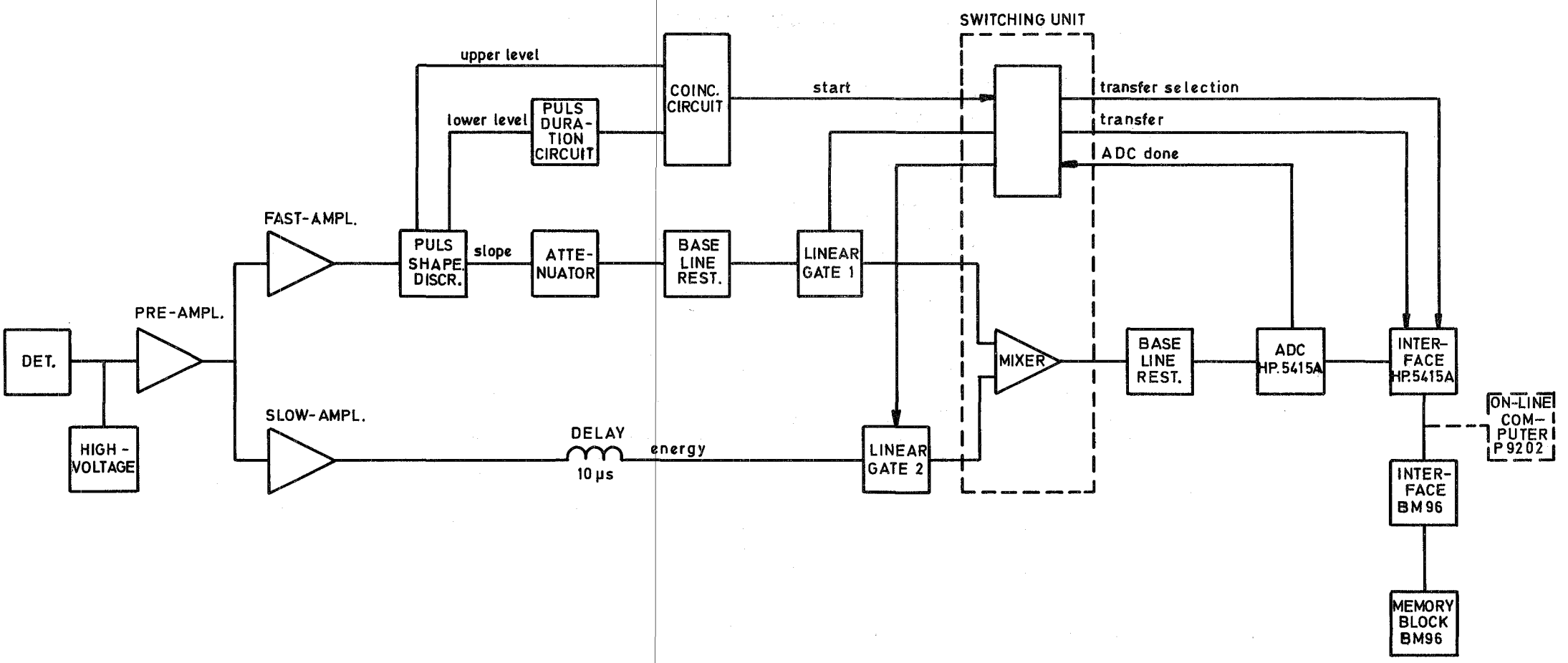
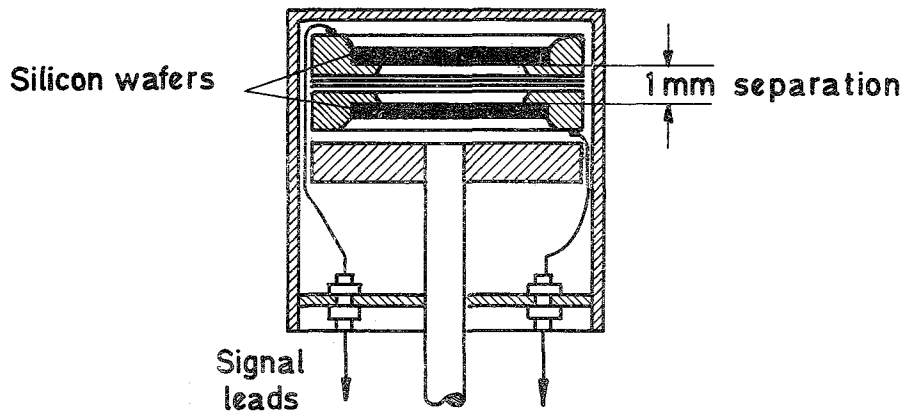


Fig. 4. KFK ${}^3\text{He}$ -SEMICONDUCTOR ELECTRONICS.



RCN PROTON RECOIL SPECTROMETER
TWO PARAMETER SET-UP WITH BM96 MEMORY BLOCK

Fig. 5.



Schematic drawing of model 780 ^3He fast neutron sandwich spectrometer head.

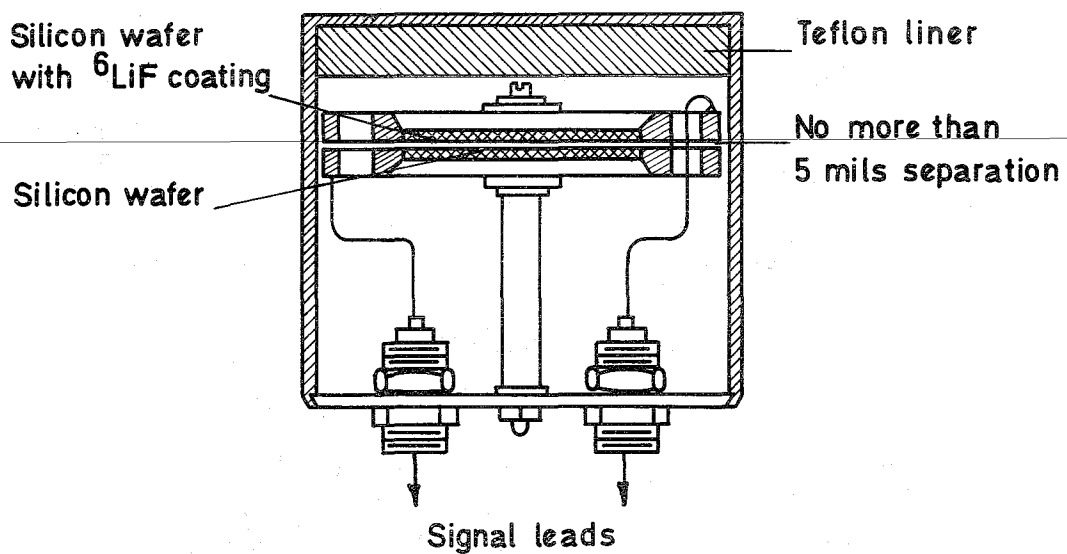


Fig. 6. Schematic drawing of model NSB 14 ^6LiF fast neutron sandwich spectrometer head.

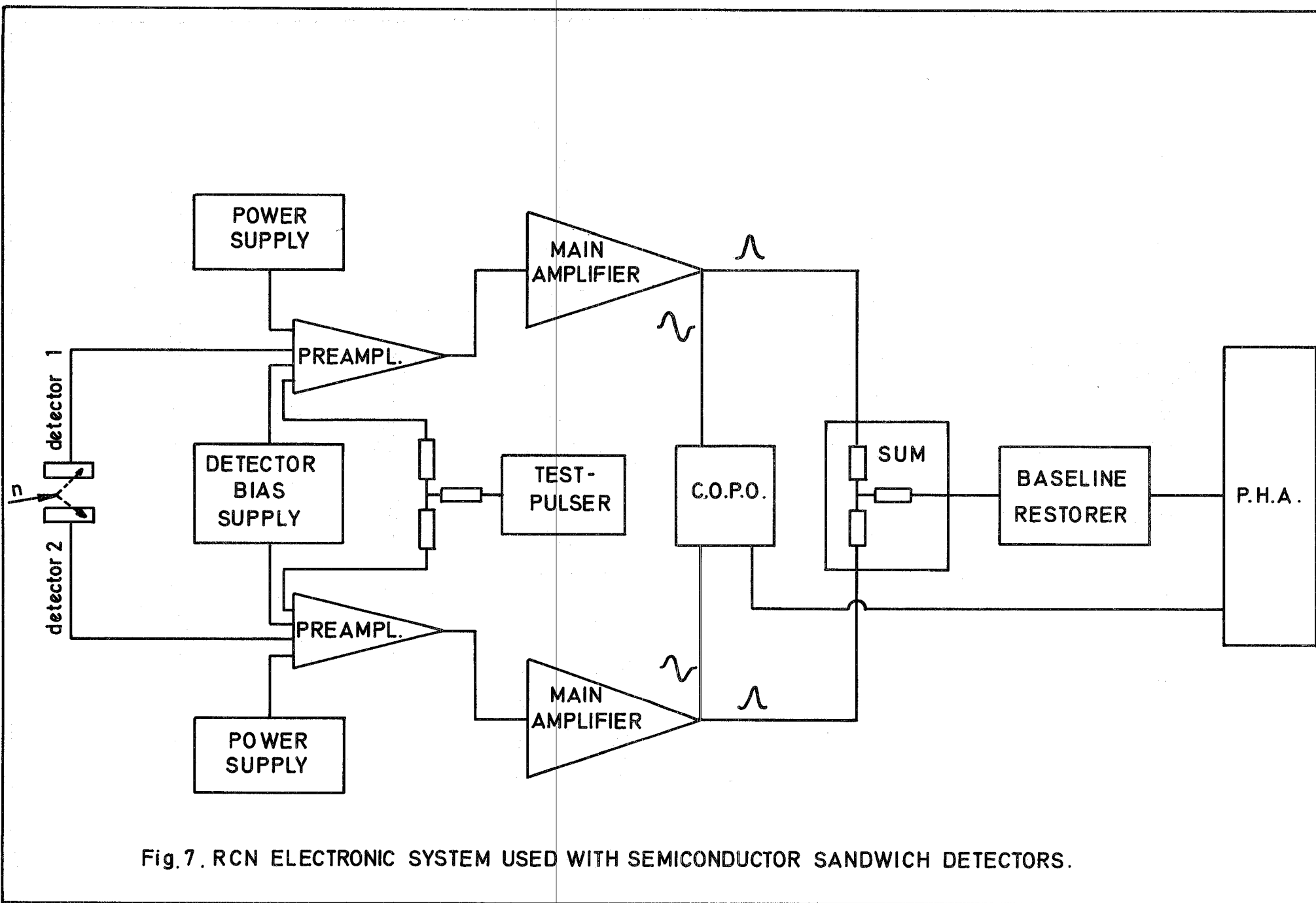


Fig. 7. RCN ELECTRONIC SYSTEM USED WITH SEMICONDUCTOR SANDWICH DETECTORS.

CEN / SCK PROTON RECOIL PROPORTIONAL COUNTER
ELECTRONICS.

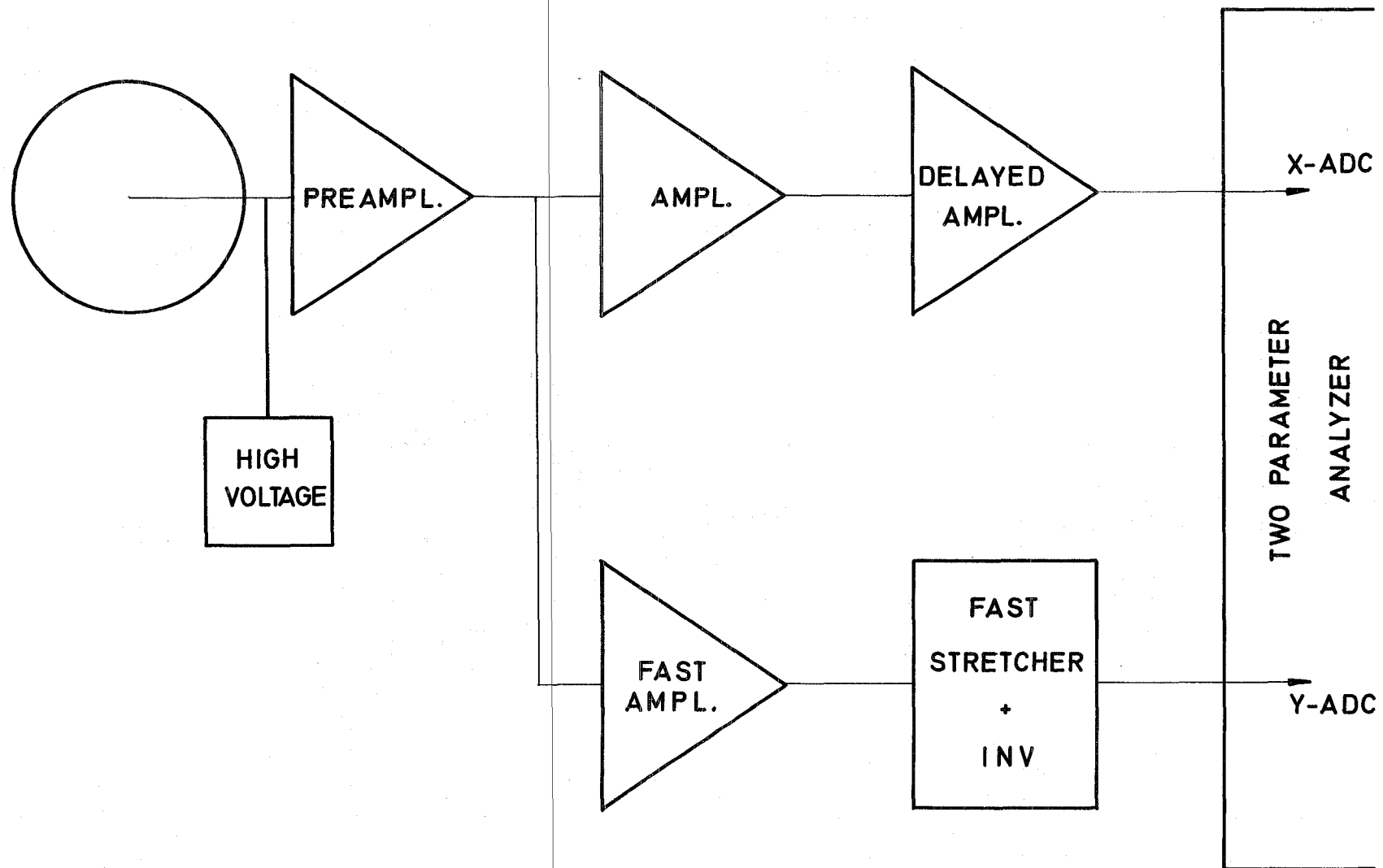
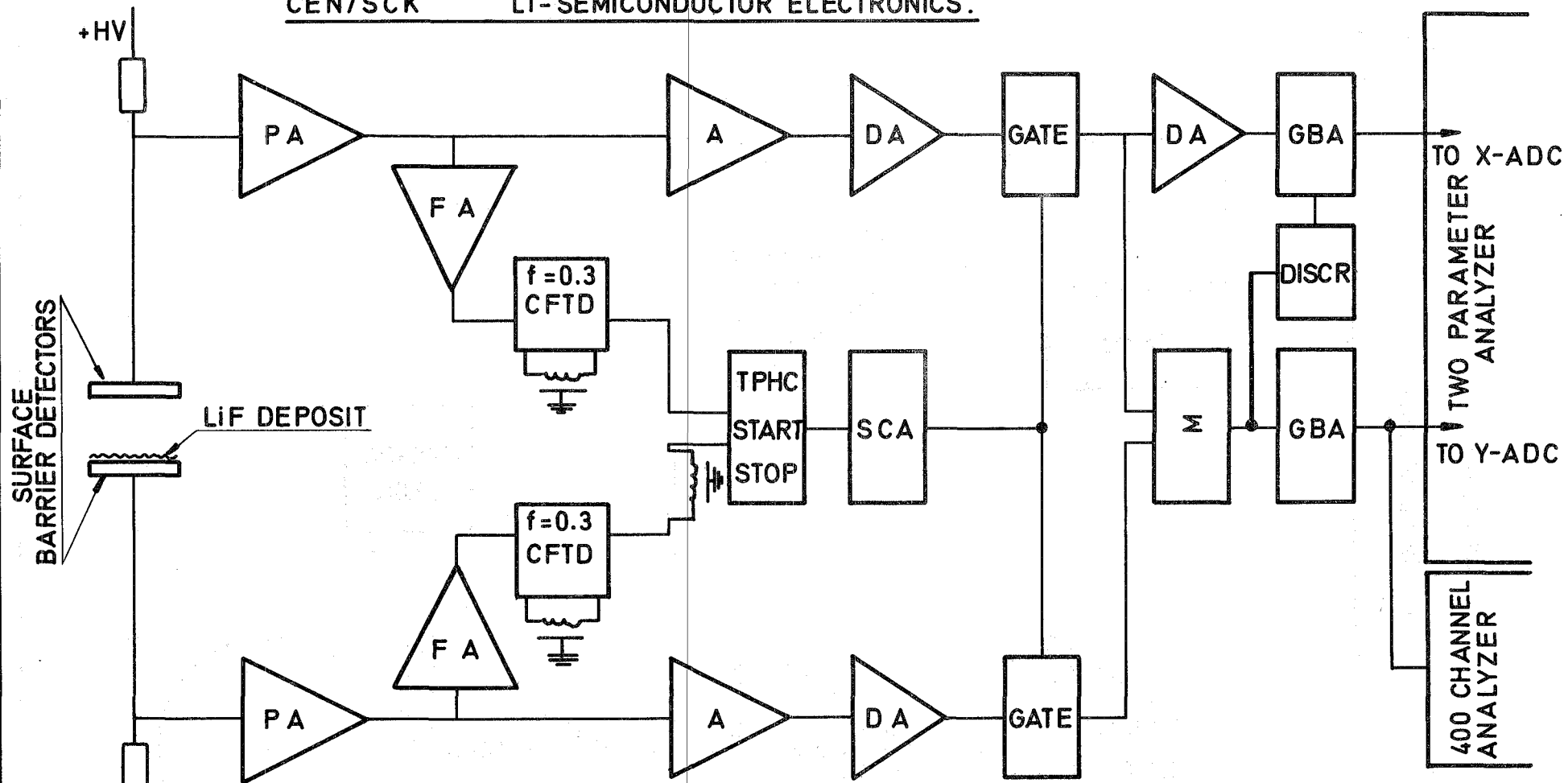


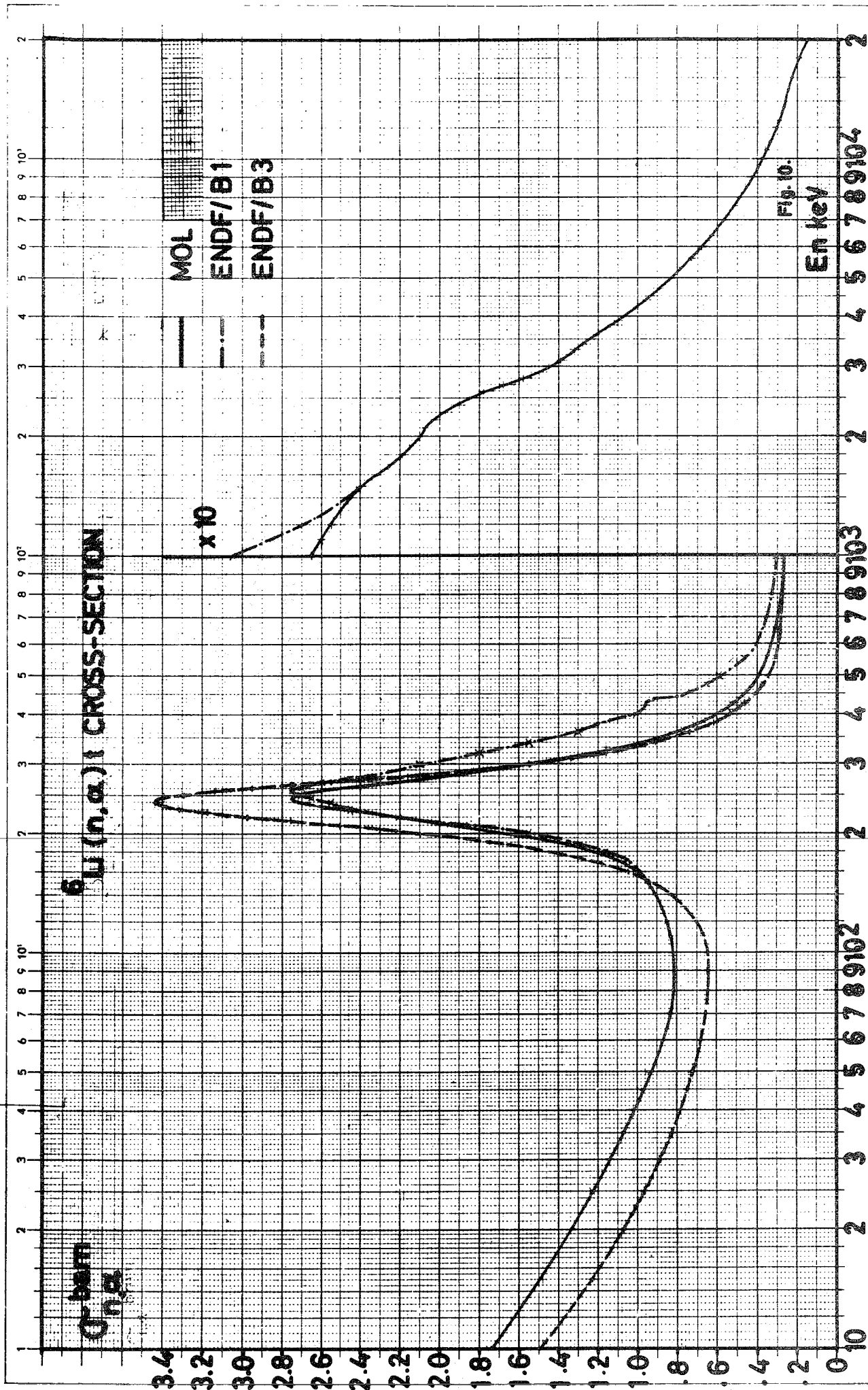
Fig .8.



+HV
 GBA : Gated biased amplifier .
 DISCR : Discriminator .
 SCA : Single channel analyser .
 Σ : Sum module .
 PA : Preamplifier .

FA : Fast amplifier .
 A : Amplifier .
 CFTD : Constant fraction timing discriminator .
 DA : Delay amplifier .
 TPHC : Time to pulse height converter .

Fig.9.



RCN NEUTRON SPECTRUM MEASUREMENT IN THE $\Sigma\Sigma$ FACILITY WITH A PROTON RECOIL SPECTROMETER

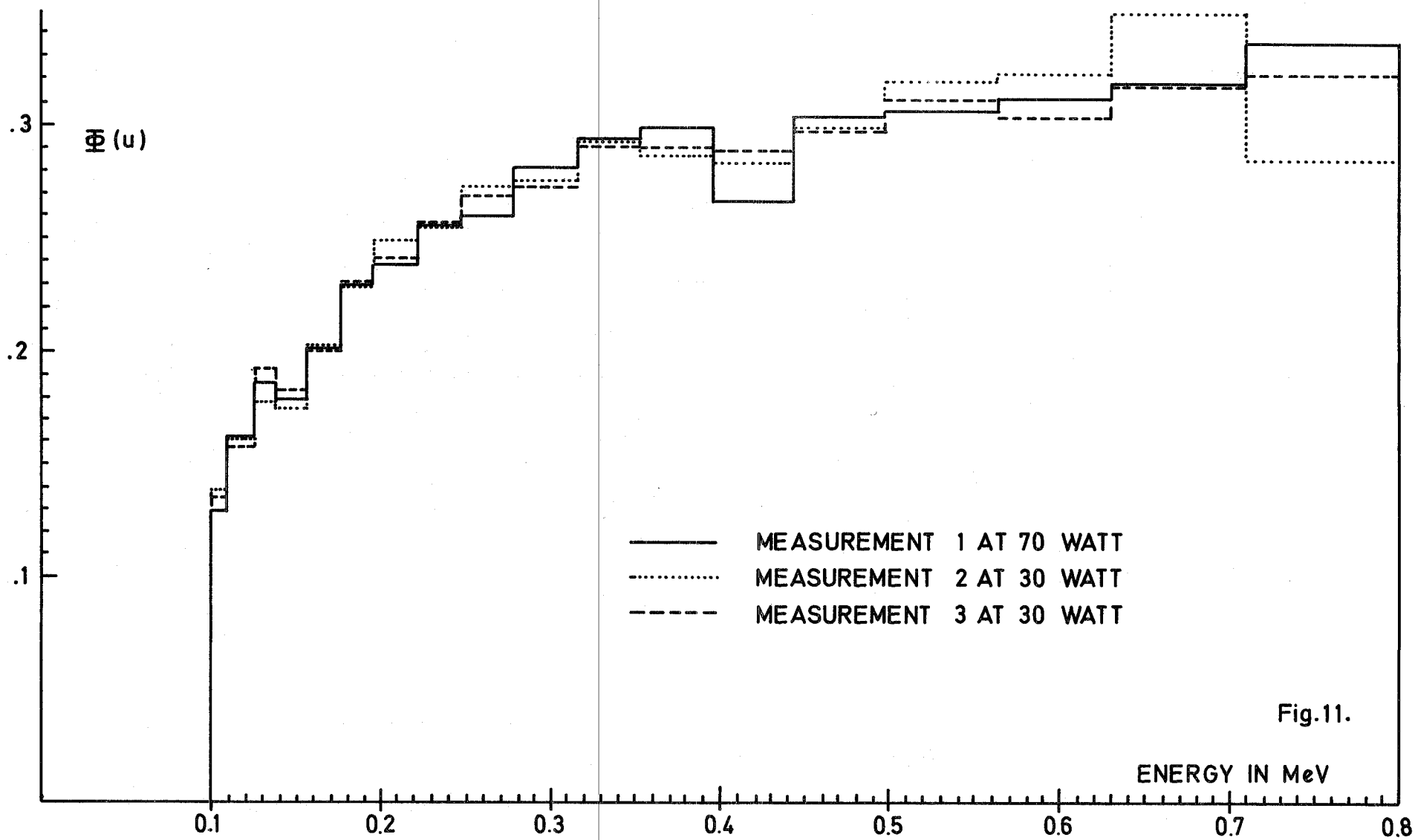


Fig.11.

(n,p) SPECTROMETRY RESULTS

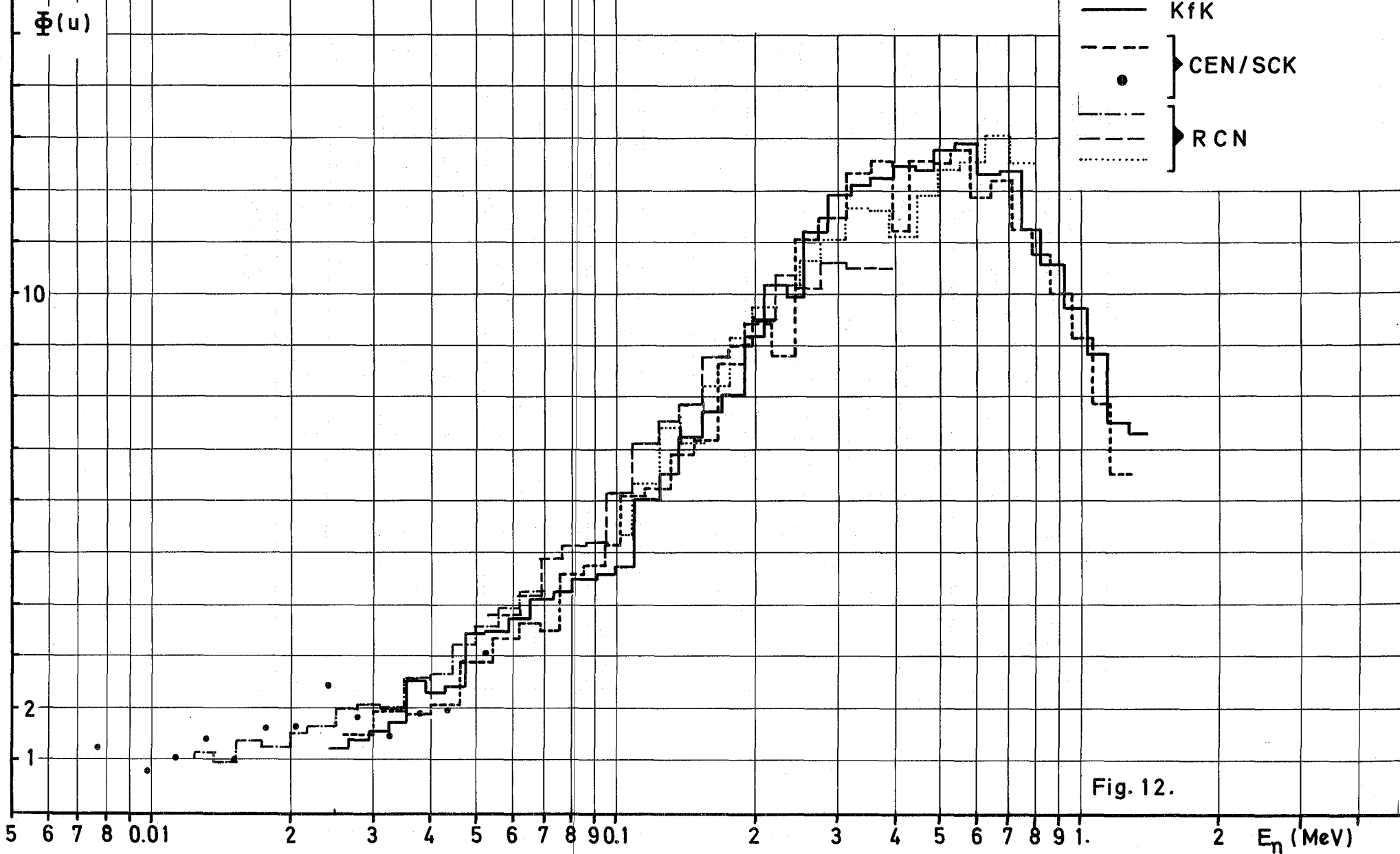


Fig. 12.

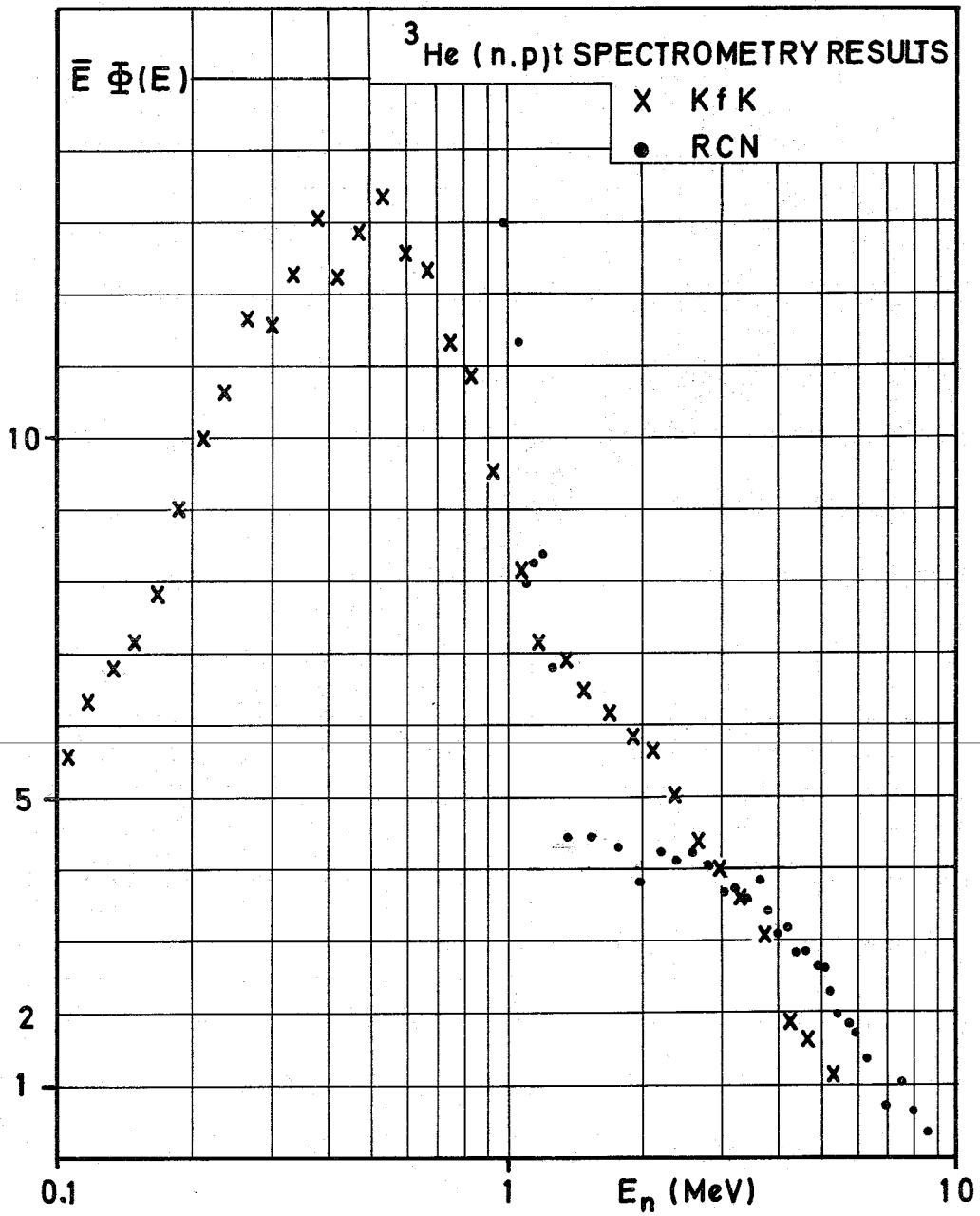


Fig. 13.

${}^6\text{Li}(n,\alpha)t$ SPECTROMETRY RESULTS

$\bar{E}\Phi(E)$

- + RCN
 - x TWO PARAMETER ANALYZER
 - 400 CHANNEL ANALYZER
- } CEN/SCK

10

5

1

0

0.1

2

3

4

5

6

7

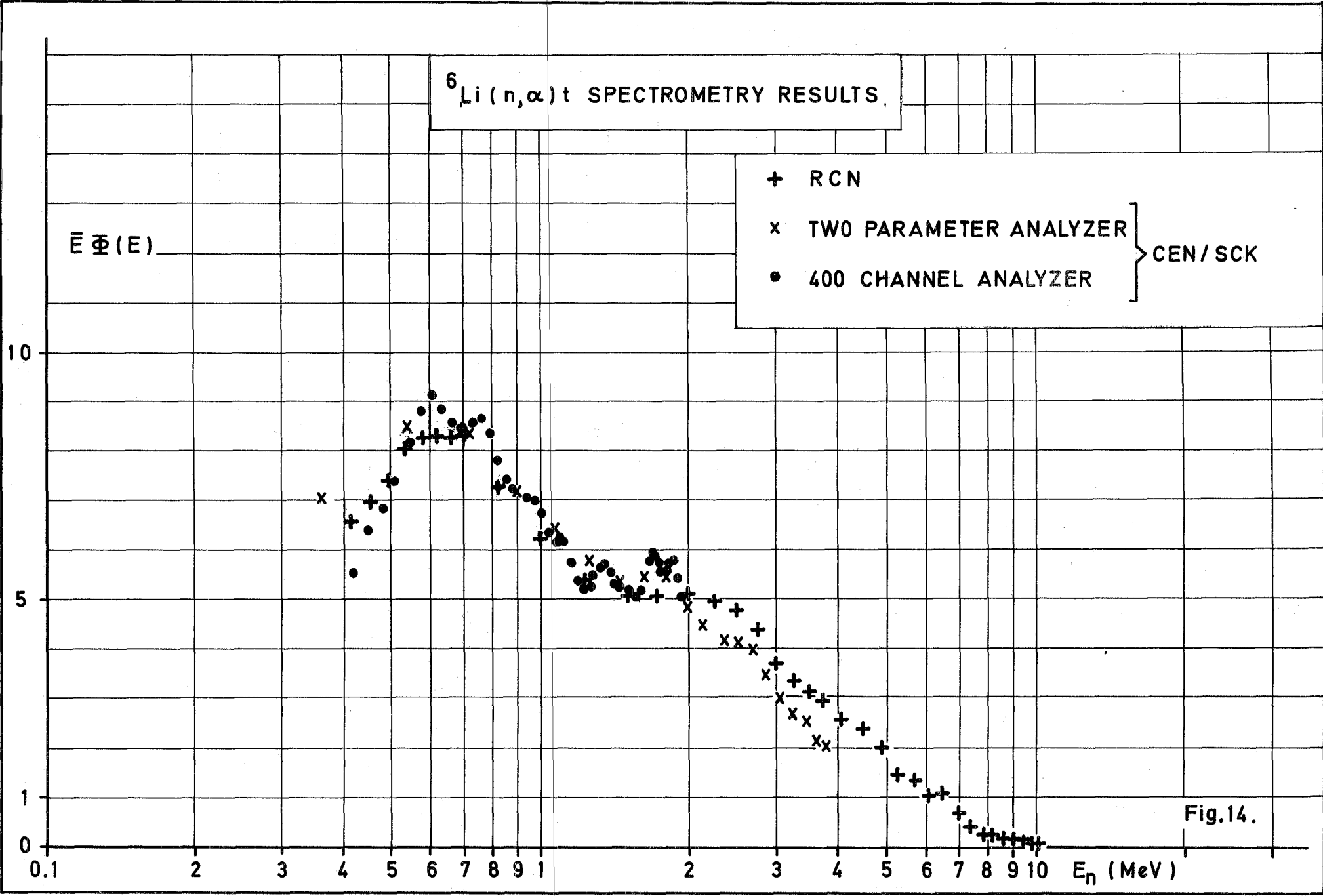
8

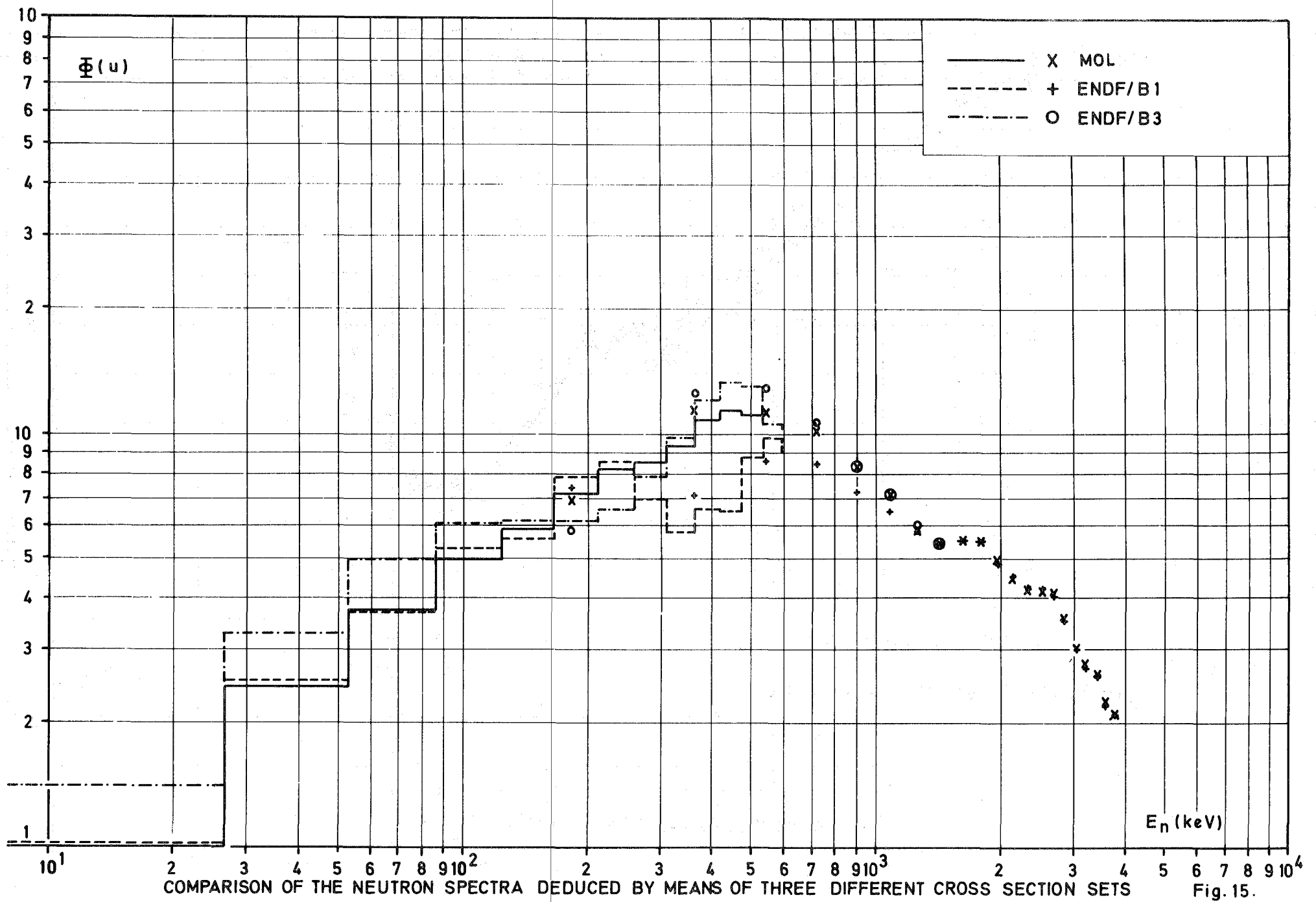
9

10

E_n (MeV)

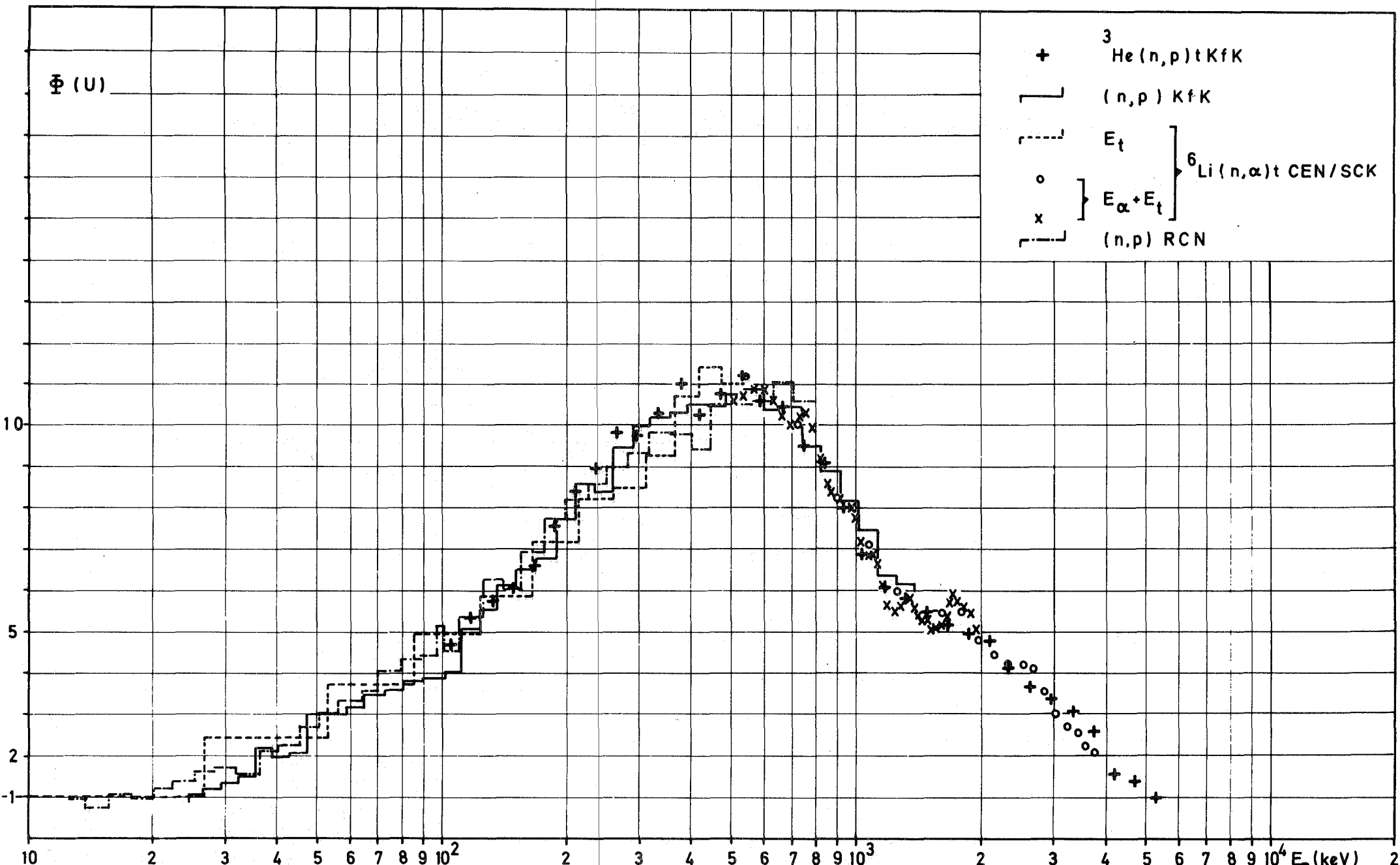
Fig.14.





COMPARISON OF THE NEUTRON SPECTRA DEDUCED BY MEANS OF THREE DIFFERENT CROSS SECTION SETS

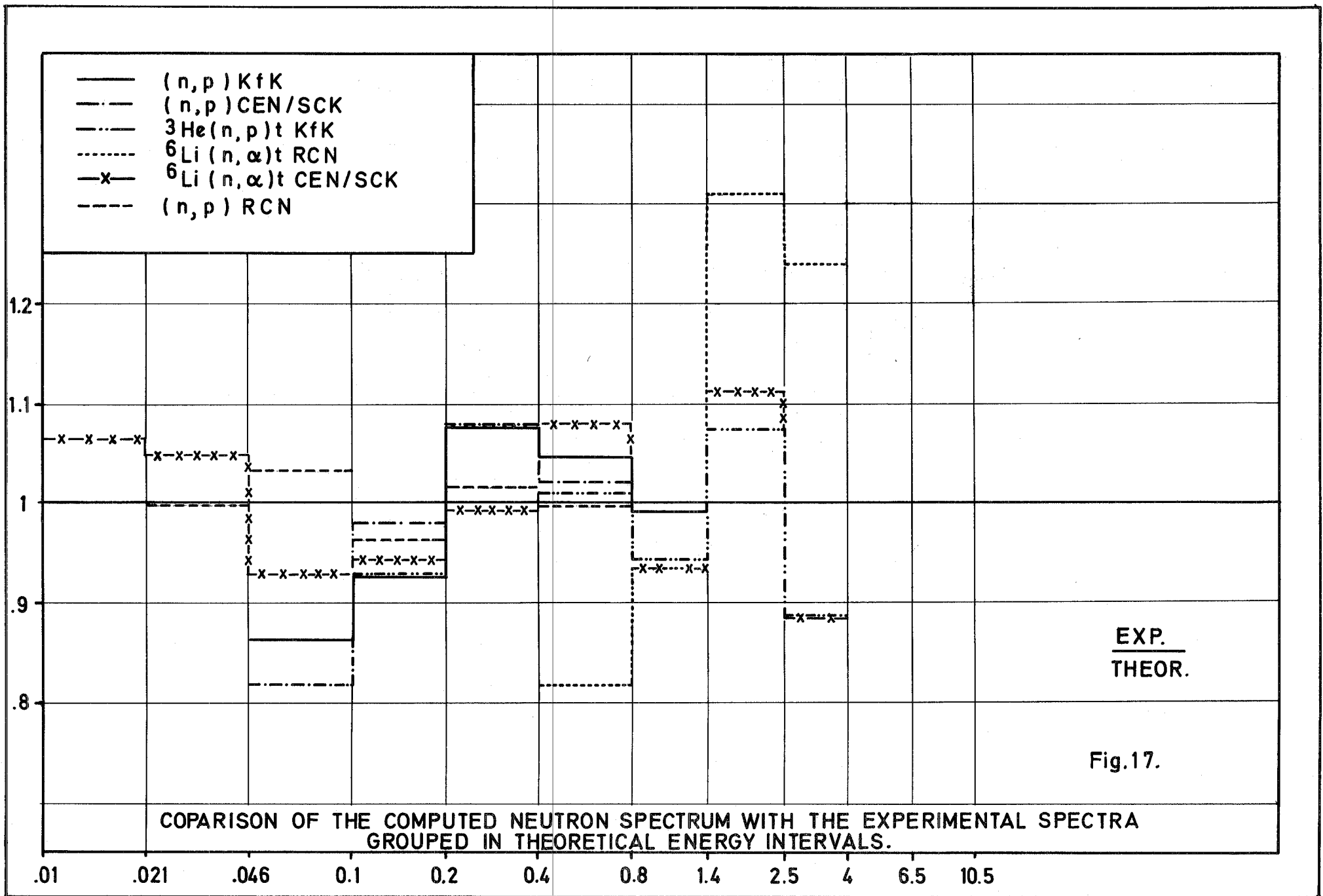
Fig. 15.



+ ${}^3\text{He}(n,p)t$ KfK
 [] (n,p) KfK
 - - - E_t
 o } $E_\alpha + E_t$
 x } ${}^6\text{Li}(n,\alpha)t$ CEN/SCK
 [] (n,p) RCN

COMPARISON OF (n,p) ${}^3\text{He}(n,p)t$ AND ${}^6\text{Li}(n,\alpha)t$ RESULTS

Fig.16.



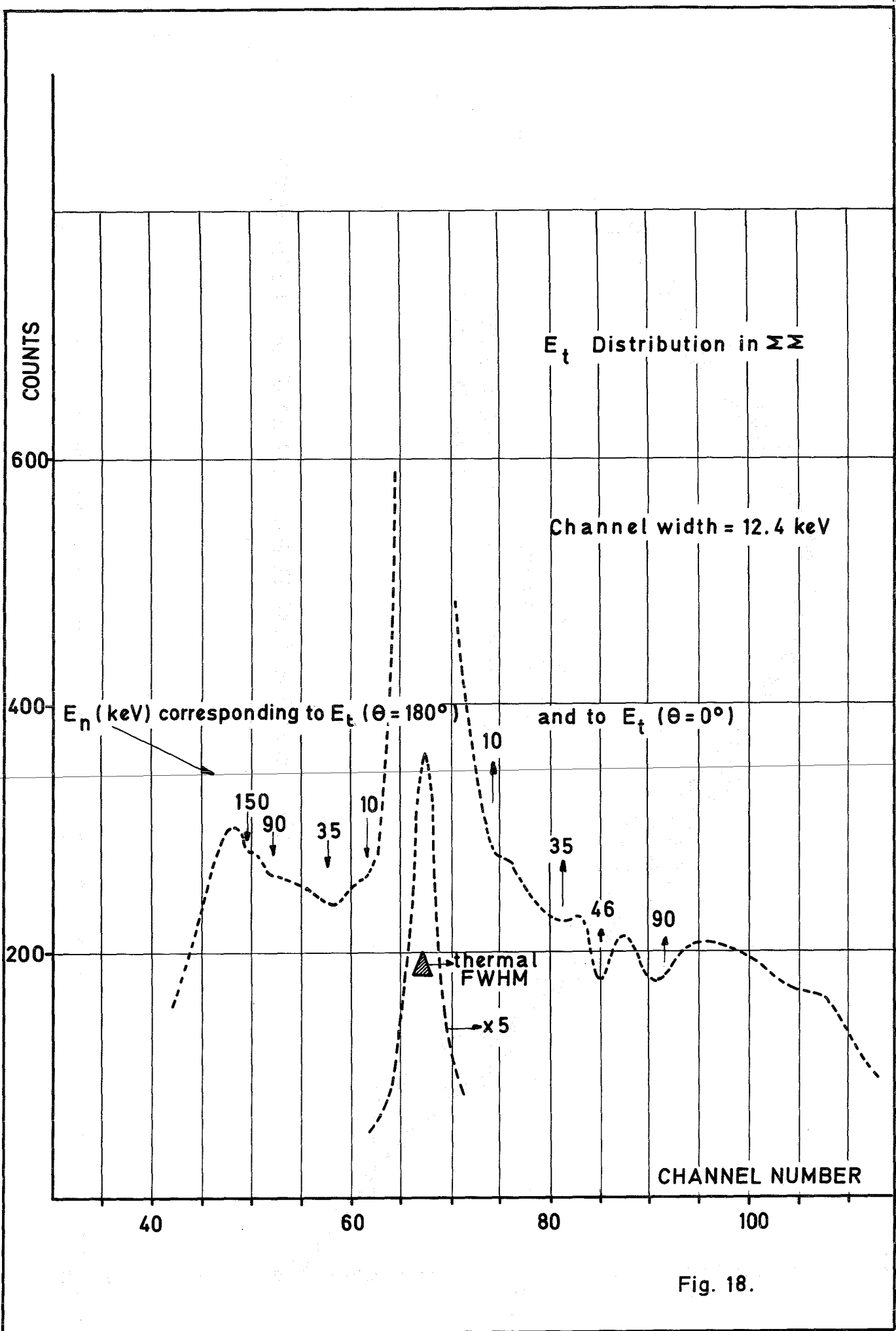


Fig. 18.

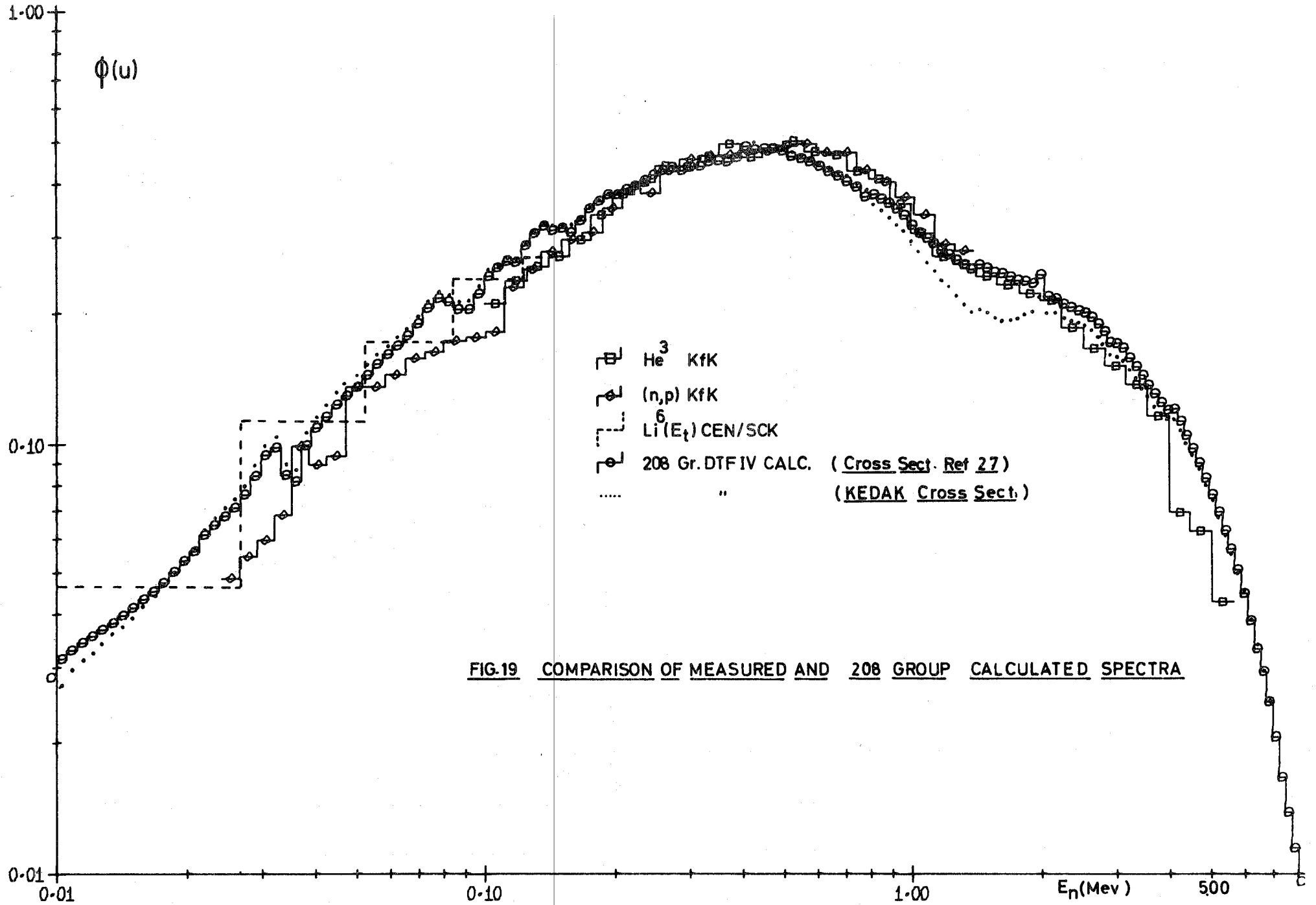


FIG.19 COMPARISON OF MEASURED AND 208 GROUP CALCULATED SPECTRA

